UNIVERSITÉ DU QUÉBEC À MONTRÉAL

NATURAL VARIABILITY OF PELAGIC AND BENTHIC CONDITIONS IN THE GULF OF ST. LAWRENCE DURING THE LATE HOLOCENE

THESIS PRESENTED
AS PARTIAL REQUIREMENT FOR
MSc. IN ENVIRONMENTAL SCIENCES

BY
NOUHA DHAHRI

NOVEMBER 2010

UNIVERSITÉ DU QUÉBEC À MONTRÉAL

VARIABILITÉ NATURELLE DES CONDITIONS PÉLAGIQUES ET BENTHIQUES DANS LE GOLFE DU SAINT-LAURENT À L'HOLOCÈNE SUPÉRIEUR

MÉMOIRE PRÉSENTÉ
COMME EXIGENCE PARIELLE
DE LA MAÎTRISE EN SCIENCES DE L'ENVIRONNEMENT

PAR
NOUHA DHAHRI

NOVEMBRE 2010

TABLE DES MATIÈRES

AVANT-PROPOS

Ce mémoire de maîtrise est présenté sous la forme d'un article scientifique qui sera soumis à la revue *Marine Micropaleontology*. Pour répondre aux exigences de cette revue, le texte a été écrit dans la langue anglaise et sa mise en forme diffère de celle recommandée par l'Université du Québec à Montréal. Les tableaux et les figures sont placés à la suite des références, alors que les annexes sont présentées à la fin du mémoire. Ma directrice de recherche Mme Anne de Vernal, chercheure et professeure au département des Sciences de la Terre et de l'Atmosphère de l'UQÀM, a participé à la rédaction de cet article.

REMERCIEMENTS

Je tiens à exprimer mes remerciements à toutes les personnes qui ont participé, à titre professionnel ou personnel, de près ou de loin, à la réalisation de ce projet de maîtrise.

Mes plus vifs remerciements vont à ma directrice de maîtrise, Mme Anne de Vernal, qui m'a chaleureusement accueillie dans son équipe de recherche et m'a offert plusieurs opportunités pour mieux connaître le milieu de recherche scientifique au Canada. Je lui suis très reconnaissante pour son bon encadrement, son attention et surtout sa serviabilité malgré les nombreuses tâches qui l'assaillent. Elle m'a constamment aidée avec ses précieux conseils en me faisant profiter de son expérience et de son savoir.

Je dois également remercier Taoufik Radi, pour son aide et ces conseils surtout dans le traitement des données, Maryse Henry, qui m'a initiée au travail dans le laboratoire de micropaléontologie et qui m'a beaucoup aidée dans l'identification des dinokystes, et Julie Leduc pour son aide et ses conseils dans l'identification des foraminifères. J'aimerai remercier également Jean-François Hélie et Agnieszka Adamowicz pour leur contribution aux analyses géochimiques et isotopiques. Merci à Bassam Ghaleb pour ses conseils et son aide avec la chronologie. Merci à tout le personnel du GEOTOP qui m'a accordé support et assistance. Merci aussi à Sophie, Benoit et Linda qui n'ont pas hésité à partager leurs connaissances avec moi. Je remercie aussi mes amies et compagnons de bureau Sarah, Caro et Nat avec qui j'ai partagé d'agréables moments.

Je tiens à remercier Mr Pierre Drapeau, professeur au département des sciences biologiques de l'UQAM, qui m'a offert la chance d'étudier à l'UQAM. Merci à Mme Sylvie De Grosbois, coordonatrice à l'institut des sciences de l'environnement, et Mr Daniel Gagnon, professeur au département des sciences biologiques de l'UQAM, pour leur support et leurs conseils.

Je remercie mes parents, papa Magtouf et maman Samira, et mes sœurs Rima, Hiba et Aya qui m'ont accordé soutien et confiance durant toute la durée de mes études et qui ont partagé les joies et satisfactions mais aussi les moments difficiles et de découragement. Sans leur soutien, ce travail n'aurait pas vu le jour.

LISTE DES FIGURES

LISTE DES TABLEAUX

RÉSUMÉ

La séquence sédimentaire de la carotte COR0503-CL05-37PC, prélevée dans le chenal Laurentien au centre du Golfe du Saint-Laurent (48°20'N - 61°29'W, à 408 m de profondeur), a fait l'objet de plusieurs analyses géochimiques et micropaléontologiques dans le but de reconstruire les variations de la productivité pélagique et des conditions du milieu benthique dans le golfe du Saint-Laurent pendant les derniers millénaires. Les analyses géochimiques (C_{org} et C_{org}/N) et isotopiques ($\delta^{13}C_{org}$ et $\delta^{15}N$) montrent des variations importantes de flux de matière organique, notamment une augmentation du taux de carbone organique, depuis environ 2300 ans cal. BP, que l'on estime être liée à l'augmentation de l'apport en matière organique d'origine marine. Les kystes des dinoflagellés permettent également de reconstruire une augmentation de la productivité biogénique dans les eaux de surface. Par ailleurs, plusieurs changements ont été enregistrés dans les assemblages de foraminifères benthiques calcaires. Ces changements se manifestent essentiellement par l'augmentation de l'abondance relative, vers 2000 ans cal. BP, de *Brizalina subaenariensis*, *Globobulimina auriculata* et *Bulimina exilis*, des espèces tolérant de faibles taux d'oxygène et des flux de carbone organique élevés. La variation de l'abondance de *Nonionellina labradorica* indique des changements dans l'apport des eaux du Courant du Labrador. En outre, les analyses isotopiques ($\delta^{18}O$) sur les tests de foraminifères benthiques *Bulimina marginata*, montrent des variations de la température et/ou de l'origine des eaux profondes qui sont indépendantes de la variation de la productivité pélagique et de l'augmentation de l'apport en matière organique.

Mots clés:
Golfe du Saint-Laurent; hypoxie; dinokystes, productivité, foraminifères benthiques, géochimie, isotopes stables, Holocène.

INTRODUCTION GÉNÉRALE

L'état de l'hypoxie, lorsque la concentration en oxygène dissous dans l'eau chute au-dessous d'un seuil létal de 2 mg L^{-1} (ou 62,5 µmol L^{-1}), est un problème alarmant dans plusieurs milieux côtiers, estuariens (Diaz et Rosenberg, 1995; 2008) et océaniques profonds (Keeling et Garcia, 2002; Gilbert *et al.*, 2010). Le nombre de régions affectées par ce problème ne cesse d'augmenter (Verity *et al.*, 2006). L'hypoxie a des conséquences graves sur la vie et l'équilibre des écosystèmes aquatiques (Diaz et Rosenberg, 1995; Wu, 2002). Elle peut affecter et menacer le métabolisme et la survie des animaux aquatiques, compromettre la capacité natatoire, influer sur la digestion, la croissance et la reproduction. Plusieurs espèces sont affectées par ce phénomène incluant des poissons d'intérêt commercial telle la morue (Chabot et Dutil, 1999; Wu, 2002). En outre, dans des conditions d'hypoxie sévère (moins de 30% de saturation en oxygène dissous), il peut se produire une mortalité massive de certaines espèces de poisson, la migration d'autres espèces ainsi que des changements de communautés favorisant l'installation des espèces les plus tolérantes (Diaz et Rosenberg, 1995 ; Wu, 2002). L'hypoxie influence donc indirectement l'abondance et la distribution de plusieurs animaux aquatiques notamment celles des espèces de grande taille, tels les tortues marines et des mammifères marins, en modifiant la disponibilité de leurs proies (Craig *et al.*, 2001).

Des études réalisées dans l'estuaire maritime du Saint-Laurent (EMSL) ainsi que dans le golfe du Saint-Laurent (GSL) mettent en évidence des changements récents de la composition physico-chimique des eaux profondes depuis le début du dernier siècle (Budgen, 1991; Gilbert *et al.*, 2005, 2007). Ces changements se manifestent par une baisse des teneurs en oxygène dissous et par l'augmentation de la température des eaux profondes le long du Chenal Laurentien (Gilbert *et al.*, 2005). Il a été démontré par des mesures directes sur la masse d'eau profonde de l'EMSL,

qu'il y a eu un réchauffement des masses d'eau de 1,7°C depuis 1930 ainsi qu'une diminution des teneurs en oxygène dissous de près de 50 %, soit de 125 µmol L^{-1} dans les années 1930 à 65 µmol L^{-1} à la fin du 20ème siècle (Gilbert *et al.*, 2005, 2007). En outre, les analyses de quelques séquences sédimentaires prélevées de l'EMSL suggèrent que la diminution des concentrations en oxygène dissous a commencé à se manifester de façon sévère dans les années 1960 (Thibodeau *et al.*, 2006). De même, dans le GSL, les observations et les données sédimentaires montrent une diminution récente de la concentration d'oxygène dissous ainsi qu'une augmentation de près de 1,9°C de la température des eaux profondes (Gilbert *al.*, 2005; Genovesi, 2009).

L'origine de l'hypoxie dans l'EMSL et le GSL peut avoir plusieurs causes. Dans le cas de l'EMSL, Thibodeau *et al.* (2006) expliquent la diminution du niveau d'oxygène dissous par l'augmentation des flux de carbone liés à l'eutrophisation anthropogénique. Les activités humaines autour du système Saint-Laurent seraient responsables de l'accroissement des décharges de nutriments issus de l'érosion et du lessivage des sols agricoles riches en fertilisants ainsi qu'aux décharges de matière organique terrigène provenant de l'industrie du papier (Thibodeau *et al.*, 2006). Ces décharges augmentent le flux de carbone et la productivité biologique dans l'eau et ont pour résultat la consommation accrue d'oxygène dissous lors de la dégradation de la matière organique dans les eaux profondes (Gilbert *et al.*, 2007; Thibodeau *et al.*, 2006). Par ailleurs, Gilbert *et al.* (2005) ont montré que la diminution du niveau d'oxygène dissous ne résulte pas uniquement de l'augmentation des flux de carbone mais qu'elle a aussi un lien avec l'augmentation de la température des eaux. Le réchauffement de l'eau a été attribué au changement des proportions relatives des eaux froides du courant du Labrador et des eaux chaudes du courant Nord Atlantique. Dans la partie centrale du GSL, Genovesi (2009) n'a pas noté d'indice probant de l'augmentation de la productivité primaire, mais ses résultats mettent en évidence un réchauffement des eaux profondes au cours des dernières décennies. Cela laisse supposer que la diminution des niveaux d'oxygène dans le GSL n'y serait pas due à

l'eutrophisation mais plutôt au changement des propriétés physiques des eaux profondes.

L'élévation de la température des eaux profondes de l'EMSL et du GSL semble être une caractéristique régionale (Thibodeau *et al.*, 2010). Elle pourrait résulter de proportions de mélange variables des eaux nord atlantiques et du Labrador à l'entrée du Chenal Laurentien (cf. Gilbert *et al.*, 2005) et être une réponse à une variabilité naturelle des conditions de circulation océanique. Il pourrait également s'agir d'une manifestation du réchauffement climatique lié aux activités anthropiques. Il est ainsi nécessaire d'étudier des séquences temporelles couvrant les derniers millénaires pour déterminer les influences respectives de la composante naturelle et du forçage anthropique. C'est dans ce contexte que nous pouvons inscrire cette étude.

Pour répondre à la question sur l'influence de la variabilité naturelle et de l'effet anthropique sur les conditions environnementales dans le GSL, nous avons essayé de reconstruire les conditions hydrographiques et la productivité des eaux profondes. Nous avons analysé le contenu d'une carotte sédimentaire COR0503-CL05-37PC prélevée dans le chenal Laurentien, au centre du golfe au même site que la carotte boîte COR0503-CL05-37BC (Genovesi, 2009), qui couvre environ deux siècles de sédimentations. À l'instar de ce qui a été fait par Genovesi (2009), nous avons utilisé une approche basée sur plusieurs traceurs pour reconstruire les conditions environnementales des derniers millénaires. Les traceurs micropaléontologiques et géochimiques ont permis d'évaluer les changements de la productivité primaire et des conditions dans les eaux profondes. Pour retracer la productivité primaire pélagique et les conditions de surface (température, salinité, couvert de glace), nous nous sommes basés sur les assemblages de dinokystes (e.g., de Vernal *et al.*, 1993, 1997, 2005; Radi et de Vernal, 2007, 2008). Les foraminifères benthiques ont été utilisés comme traceurs des conditions des eaux profondes (Murray, 2001; Jorissen *et al.*, 2007). Les assemblages et l'abondance des foraminifères benthiques sont utilisés comme indicateurs de la productivité benthique, des flux de carbone organique et de concentration en oxygène dissous

(e.g., den Dulk *et al.*, 2000; Osterman, 2003; Osterman *et al.*, 2009). Par ailleurs, la composition isotopique ($\delta^{18}O$ and $\delta^{13}C$) des tests de foraminifères benthiques est utilisée pour retracer les caractéristiques des eaux dans lesquelles leurs tests carbonatés se sont précipités. La composition isotopique fournit en effet des informations sur les conditions de température et de salinité des eaux (e.g., Waelbroeck *et al.*, 2002; Ravelo et Hillaire-Marcel, 2007). Pour déterminer l'origine de la matière organique piégée dans les sédiments, nous avons par ailleurs effectué diverses analyses géochimiques (teneur en carbone organique et le rapport C_{org}/N) et isotopiques ($\delta^{13}C$ et $\delta^{15}N$) (e.g., Meyers, 1994, 1997; Muzuka et Hillaire-Marcel, 1997; McKay *et al.*, 2004).

CHAPITRE 1

NATURAL VARIABILITY OF PELAGIC AND BENTHIC CONDITIONS IN THE GULF OF ST. LAWRENCE DURING THE LATE HOLOCENE

Nouha Dhahri[1,*], Anne de Vernal[1]

[1] GEOTOP: Centre de recherche en Géochimie Isotopique et en Géochronologie, Université du Québec à Montréal, C.P. 8888, Succ. Centre-Ville, Montréal, Québec, Canada, H3C 3P8. Tel : + 1-514-987-4080; Fax : +1-514-987-3635

[*]Corresponding author: E-mail: nouha1dhahri@yahoo.fr

Abstract

A sedimentary section from core COR0503-CL05-37PC, collected in the Laurentian Channel in the central part of the Gulf of St. Lawrence (48°20'N - 61°29'W, at 408 water depth), was analyzed for its geochemical and micropaleontological content in order to reconstruct variations in pelagic productivity and bottom water conditions in the Gulf of St. Lawrence during the last millennia. Geochemical (C_{org} and C_{org}/N) and isotopic results ($\delta^{13}C_{org}$ and $\delta^{15}N$) reveal important variations of organic matter flux and an increase of organic carbon content since 2300 cal. years BP, which could be related to the increase of marine organic matter input. Similarly, the dinocyst assemblages suggest also a significant increase of biogenic productivity since about 2300 cal. years BP in the upper water mass. Moreover, changes are recorded in benthic foraminiferal assemblages. An increase, since 2000 cal. years BP, of the abundances of *Brizalina subaenariensis*, *Globobulimina auriculata* and *Bulimina exilis* in the upper part of the studied sector reveals a trend toward a low oxygen level and high organic input. The variation of the relative abundance of *Nonionellina labradorica* also suggests concomitant decrease in the contribution of Labrador Current Water. The isotopic analyses performed on *Bulimina marginata* shells also suggest variations of bottom water temperatures. The results show that important changes of environmental conditions occurred at a millennial scale as part of natural variation in a complex ecosystem.

Key Words: Gulf of St. Lawrence; hypoxia; dinocyst, productivity, benthic foraminifera; geochemistry, stable isotopes, Holocene.

1.1. Introduction

Hypoxia, defined as the dissolved oxygen concentration below 62.5 µmol L^{-1}, is an alarming problem that occurs in many coastal and estuarine environments (Diaz and Rosenberg, 1995; 2008). It is suggested that the recent decrease of dissolved oxygen concentrations also occurs in the deep ocean (Keeling and Garcia, 2002; Gilbert *et al.*, 2010). The number of hypoxic zones has been increasing around the world (Verity *et al.*, 2006). Hypoxia has many impacts on aquatic organisms and causes severe ecosystem disturbance (Diaz and Rosenberg, 1995, Wu, 2002). It affects the growth, reproduction and digestion of many organisms (Wu, 2002) including species of commercial fisheries importance such as Atlantic cod (Chabot and Dutil, 1999). Moreover, hypoxia has an effect on the distribution and abundance of large aquatic animals such as sea turtles and marine mammals by changing the availability of their prey (Craig *et al.*, 2001).

Since the beginning of the last century, changes in the physical and chemical composition of the bottom waters have been recorded in the Lower St. Lawrence Estuary (LSLE) and the Gulf of St. Lawrence (GSL) (Budgen, 1991; Gilbert *et al.*, 2005, 2007). It was observed that about 1300 km^2 of Laurentian Channel (LC) are bathed by hypoxic and warmer bottom waters (Gilbert *et al.*, 2005). Direct measurements of the bottom waters of the LSLE have shown a significant warming of about 1.7°C since the 1930s and a remarkable decrease of dissolved oxygen concentration from 125 µmol L^{-1} in the 1930s to 65 µmol L^{-1} at the end of the 20^{th} century (Gilbert *et al.*, 2005, 2007). Analyses of sedimentary sequences from the LSLE suggest that the decrease of dissolved oxygen concentrations have started since the 1960s (Thibodeau *et al.*, 2006). Similarly, in the GSL, both observation and sedimentary data suggest recent diminution of the dissolved oxygen concentration and about 1.9°C warming (Gilbert *al.*, 2005; Genovesi, 2009).

There are several factors that may be contributing to the hypoxic conditions in the LSLE and in the GSL. In the case of the LSLE, Thibodeau *et al.* (2006) explained

the decrease of the dissolved oxygen concentration by the increase of carbon flux related to anthropogenic eutrophication. Human activity in the St. Lawrence watershed enhanced nutrient discharges with agriculture fertilizers and terrigenous organic carbon related to waste produced by the paper mill industry. These anthropogenic discharges caused an increase in biological productivity, carbon fluxes to the sea floor and consumption of dissolved oxygen in the bottom water through organic matter degradation (Gilbert *et al.,* 2007; Thibodeau *et al.*, 2006). However, Gilbert *et al.* (2005, 2007) have shown that the increase in carbon flux cannot entirely explain the decrease in the dissolved oxygen concentrations and that hypoxia is also related to the increase in bottom water temperatures. Bottom water warming has been attributed to changes in relative proportions of the Labrador Current Water (LCW) and the North Atlantic Central Water (NACW). However in the central part of the GSL, Genovesi (2009) found no evidence of an increase in primary production, whereas increased bottom water temperature close to 2°C seems to be a significant feature of the last century. This led to the conclusion that the recent decrease in dissolved oxygen concentration in the GSL cannot be explained by eutrophication but rather by changes in the properties of bottom water masses.

The warming in bottom waters of the LSLE and GSL seems to be a conspicuous feature on a regional scale (cf. Thibodeau *et al.*, 2010). It could be related to changes in temperature due to variations in the proportion of Atlantic versus Labrador Sea waters that enter the Laurentian Channel through Cabot Strait as suggested by Gilbert *et al.* (2005). Such variations could be a response to natural variability, but the recent change could also be considered as a manifestation of the anthropogenically driven climate warming. In order to determine the respective influence of the natural variability and anthropogenic forcing, the study of time series that covers several millennia is needed. This is the main purpose of this study.

In this paper, we reconstruct hydrographical conditions and productivity of bottom waters from the analysis of sediment recovered in the piston core COR0503-CL05-37PC (hereafter COR503-37PC). This core was collected in the Laurentian

Channel, in the central part of the GSL, at the same location as box core COR0503-CL05-37BC (hereafter COR503-37BC) studied by Genovesi (2009; Genovesi *et al.*, submitted) that encompasses the last two centuries. This study is thus complementary to the work undertaken by Genovesi (2009) as it focuses on longer time series. A multi-proxy approach has been used in order to reconstruct the environmental conditions in the GSL during the last millennia following the same procedures described by Genovesi (2009). Micropaleontological and geochemical proxies have been used to evaluate changes in primary productivity and hydrographical conditions of bottom water in the GSL. To reconstruct the primary pelagic productivity, we used dinoflagellate cysts assemblages as indicators of sea surface conditions such as temperature, salinity and sea-ice cover (e.g., de Vernal *et al.*, 1993, 1997, 2005; Radi and de Vernal, 2007, 2008). Benthic foraminifera were used as proxies of the bottom water conditions (Murray, 2001; Jorissen *et al.*, 2007). The assemblages and abundances of benthic foraminifera were used to document the dissolved oxygen concentration and organic carbon fluxes as they are tracers of the benthic productivity of their ecosystem (e.g., den Dulk *et al.*, 2000; Osterman, 2003; Osterman *et al.*, 2009). The isotopic compositions of their shells ($\delta^{18}O$ and $\delta^{13}C$) were also used to document physical conditions in the waters in which they calcified, notably to provide an indication of deep water temperature and salinity (e.g., Waelbroeck *et al.*, 2002; Ravelo and Hillaire-Marcel, 2007). Geochemical measurements (organic carbon C_{org} and the ratio C_{org}/N) and isotopic measurements ($\delta^{13}C_{org}$ and $\delta^{15}N$) were used to identify the origin of organic matter preserved in the sediment (e.g., Meyers, 1994, 1997; Muzuka and Hillaire-Marcel, 1997; McKay *et al.*, 2004).

1.2. Study area

1.2.1. Topography and bathymetry

The Gulf of St-Lawrence is a highly stratified 226 000 km^2 semi-enclosed sea located in eastern Canada with a water volume of about 35 000 km^3 and an average

water depth of approximately 152 m (Dickie and Trites, 1983). It has two connections with the North Atlantic Ocean: Cabot Strait to the South and the Strait of Belle Isle to the East (Fig.1). The main passage that allows major water exchanges with the North Atlantic is Cabot Strait, along the LC, which has a maximum depth of 480 m and a width of 104 km (Dickie and Trites, 1983). The Strait of Belle Isle, in northeastern the GSL, is a small passage, 16 km wide and 60 m deep (Dickie and Trites, 1983; Bugden, 1991).

The bathymetry of the GSL is marked by the LC as the dominant topographic feature of the maritime and estuarine systems in the GSL. It is a deep central trough that maintains a depth of over 300 m through the most of its 1100 km length, which extends from the continental shelf off Cabot Strait in the North Atlantic to Tadoussac in the St. Lawrence Estuary (Bugden, 1991). In the North of the GSL, the LC is ramified into two secondary branches: the Esquimans Channel and Anticosti Channel with a maximum depth of 345 m and 296 m respectively (Loring and Nota, 1973) (Fig.1).

1.2.2. Water circulation and hydrographical characteristics

The surface waters in the GSL are fed by freshwater runoff of the St. Lawrence River that drains a large watershed including that of the Great Lakes (Dickie and Trites, 1983). This freshwater discharge mixes partially with oceanic waters and flows seaward to finally exits towards the Atlantic Ocean. The surface circulation also follows the dominant wind patterns that are controlled by general cyclonic circulation (El-Sabh, 1973). The Cabot Strait allows important exchanges between the GSL and the Atlantic Ocean and thus serves as the exit for nutrient rich freshwaters. Cabot Strait also allows the input of deep oceanic waters along the LC (Saucier *et al.*, 2003). Thus the water column of the LC is divided into three layers (Dickie and Trites, 1983). A thin surface layer (approximately 50 m) characterized by low salinity (27 to 32 psu) shows a large seasonal variation in temperatures (Dickie and Trites, 1983). This layer is influenced by the vernal changes in surface flux and

freshwater discharge (Bugden, 1991). An intermediate layer extending down to 150 m is characterized by moderate salinity (31.5 to 33 psu) and very cold water (-0.5 to 1°C). This cold intermediate layer originates from winter cooling and water density increase in addition to brine release during sea-ice formation (e.g., Gilbert and Pettigrew, 1997). The bottom water layer is warmer (4 to 6°C) and saltier (~34.6 psu) than the cold intermediate layer (Dickie and Trites, 1983). The bottom water penetrates into the Gulf through Cabot Strait and results from mixing Labrador Current Water (LCW) and North Atlantic Central Water (NACW) (Gilbert *et al.*, 2005). This dense bottom water layer circulates landward. From Cabot Strait to the head of the Laurentian Channel, this layer is marked by the decrease in dissolved oxygen concentrations related to the decomposition of organic matter within the deep layer (Savenkoff *et al.*, 1996; Gilbert *et al.*, 2005).

1.3. Material and Methods

1.3.1. Sampling

The core COR503-37PC was recovered in 2005 on the *Coriolis II* using a modified version of a Benthos^{TM} piston corer that allows collecting cores up to 9 m in length and 10 cm in diameter. COR503-37PC is 7.90 m long. It was retrieved from 408 m water depth in the Laurentian Channel (48°20.0110'N - 61°29.9950'W). Core handling caused a disturbance of approximately 30 cm of sediment in the upper part of the core. Subsampling was done from 30 cm to 100 cm at 2-cm interval, and at 4-cm interval down to the base of the studied section (176 cm) of the core.

1.3.2. Chronology

The stratigraphic framework of core COR503-37PC has been established by Barletta *et al.* (2010). It was based on 5 AMS (Accelator Mass Spectrometry) ^{14}C measurements of shell fragments and paleomagnetic intensity measurements. In addition, we sampled and dated bivalve shell fragments at 45 cm. This provides a

total of 6 radiocarbon ages (Table 1). In order to convert the ^{14}C conventional age to calendar years, Barletta *et al.* (2010) calibrated the dates with the CALIB 5.0.2 software (Stuiver *et al.*, 2005) after a normalization for a $\delta^{13}C$ of −25‰ PDB and assuming a standard reservoir correction of 400 years (Hughen, *et al.*, 2004). We followed the same procedure with the sixth radiocarbon date.

1.3.3. Geochemical analyses

1.3.3.1. Sediment Carbon and Nitrogen analyses (%C_{org}, C_{org}/N, $\delta^{13}C$, $\delta^{15}N$)

Approximately 8 g of dried and crushed sediments from each sample was placed in tin cups and analysed with a Carlo Erba™ NC 2500 elemental analyzer to determine the weight percent total carbon (C_{Tot}) and total nitrogen (N_{Tot}) contents. The organic carbon content (C_{org}) was measured from sediments acidified by the fumigation method (Hélie, 2009). Subsamples were weighed into silver cups and placed carefully in a clean Teflon tray. The tray was put in a closed glass container with a beaker of concentrated HCl for 24 hours. During this interval, the HCl that saturated the air in the container reacted with the carbonate minerals. After fumigation, the silver cups were closed, wrapped in tin cups and then analyzed with Carlo Erba™ NC 2500 elemental analyzer. The results are given in percent (%) of the total weight. Replicate measurements of organic analytical reference materials determined the analytical precision which is estimated at ± 0.1 % for C_{org} and ± 0.3% for N.

The isotopic analyses of organic carbon (C_{org}), were measured on subsamples prepared following the same method used for organic carbon content (C_{org}). For isotopic analysis of total nitrogen ($\delta^{15}N_{Tot}$), we placed sediments in tin cups to be analysed. The measurements were performed with a Micromass Isoprime™ mass spectrometer coupled with a Carlo Erba™ elemental analyzer. The results are reported in δ notation (‰) with reference to V-PDB (Vienna Pee Dee *Belemnitella*)

for $\delta^{13}C$ (Coplen, 1995) and air for $\delta^{15}N$. The analytical uncertainty is 0.1 ‰ for ^{13}C and 0.2 ‰ for $\delta^{15}N$ as determined from replicate measurements of standard materials during analytical runs.

1.3.3.2. Oxygen and carbon isotopes analyses in benthic foraminiferal shells ($\delta^{18}O$, $\delta^{13}C$)

A preliminary assessment suggested that *Bulimina marginata* and *Bulimina exilis* are the most abundant and frequent species of calcareous benthic foraminifera within our samples. Tests were conducted to determine which species was most suitable for oxygen and carbon isotope analysis ($\delta^{18}O$, $\delta^{13}C$). As presented in the results section, both species yield comparable isotope compositions with respect to $\delta^{18}O$ but differ in their $\delta^{13}C$, likely due to depth habitat in the sediment (Corliss, 1985). *Bulimina marginata* is described as an intermediate infaunal species that lives near the sediment-water interface (Jorissen *et al.*, 1998), whereas *Bulimina exilis* is a deep dwelling infaunal species (Jorissen, 1999). Thus, in order to produce results that reflect better the isotopic composition of the bottom waters, in which benthic foraminifera tests are calcified, we chose to analyse $\delta^{18}O$ and $\delta^{13}C$ of *Bulimina marginata.*

Approximately one dozen calcareous tests of *Bulimina marginata* were hand picked from the 125-250 µm fraction of each subsample. The tests were roasted under vacuum at 250°C for approximately one hour. They were then analyzed with a Micromass Isoprime™ isotope ratio mass spectrometer in dual inlet mode coupled with a MultiCarb™ preparation system. To extract the CO_2, samples were acidified with pure H_3P0_4 at 90°C. Measurements were corrected to an internal reference carbonate material calibrated against the V-PDB scale. The analytical reproducibility determined by replicate measurements of the internal reference material is regularly better than 0.05 ‰.

1.3.4. Micropaleontological analyses

Prior to analysing the micropaleontological content of the sediment, subsamples were treated according to the method described by de Vernal et *al.* (1996).

For each subsample, a volume of 5 cm^3 of wet sediment was sieved on 106 µm and 10 µm mesh sieves to eliminate coarse sand, clay and fine silt particles. To dissolve carbonate and silica particles, the fraction between 10 and 106 µm was treated with warm hydrochloric acid (HCl 10%) and warm hydrofluoric acid (HF 49%). The residue was washed on a 10 µm sieve to eliminate remaining particles after the chemical treatments. The residue was mounted between slide and cover-slide in glycerine gel for optical microscopic analysis at 400x magnification. All the palynomorphs (dinocysts, pollen grains, spores and organic linings) were identified and counted. On average, 300 dinocyst specimens were identified and counted following the taxonomical nomenclature of Rochon *et al.* (1999). Concentrations of dinocysts (cysts g^{-1}) and other palynomorphs were calculated using the marker grain method (Matthews, 1969). In this paper, we only report dinocyst concentrations and the relative abundance of the most abundant dinocyt taxa. Detailed palynological data are reported in Dhahri (2010).

To quantitatively reconstruct sea-surface conditions (temperature, salinity and ice cover) and productivity, we applied the best analogue technique (Guiot and de Vernal, 2007) using the n= 1429 dinocyst reference data base and the MODerate resolution Imaging Spectroradiometer (MODIS) database (http://daac.gsfc.nasa.gov ; Behrenfeld and Falkowski, 1997) as a reference of the modern productivity. The validation exercise indicates an accuracy of reconstruction of ± 54.97 gC m^{-2}. Details about the approach can be found in Radi and de Vernal (2008).

In order to obtain sufficient quantities of benthic foraminiferal specimens for the analyses of population and isotopic measurements, a volume averaging 15 cm^3 of wet sediment was dried at room temperature. This volume was weighed and washed on 106 µm mesh sieves. The fraction >106 µm was dried, weighed and examined

with a binocular microscope (x40). All the benthic foraminiferal tests were hand-picked from the >125 μm size fraction, identified and counted in order to obtain sufficient numbers of specimens for our analyses. An average of 53 shells was collected per sample. The identification of benthic foraminifera was based on the taxonomy established by Rodrigues (1980). Here, we illustrate benthic foraminiferal concentrations (tests g^{-1}) and relative abundances of all the taxa.

1.4 Results

1.4.1 Chronology

An interpolation function, based on 5 AMS ^{14}C dates, was used by Barletta *et al,* (2010) to make up the age vs. depth relationship. According to this relationship, the sedimentation rate changes from ~190 cm kyr^{-1} to ~40 cm kyr^{-1} at about 8500 cal. years BP (i.e. ~ 375 cm) (Fig.2a). As shown in Figure 2a, the additional date obtained at 45 cm seems inconsistent with the uppermost age from shells collected at 38 cm and offset with respect to the age-depth relationship established by Barletta *et al.* (2010). Due to the disturbance in the upper part of the core and the unknown identity (habitat depth) of shells dated, we decided to use a linear regression across the few data points to estimate sedimentation rates. After adding the AMS ^{14}C date from shells collected at 45 cm (this study), we estimated that sedimentation rates in the upper part of the core average 41cm kyr^{-1}. However, according to this relationship, the upper 18 cm of the core would have unrealistic ages in the future.

In order to obtain an age-depth relationship with realistic ages, we applied across the data points linear regression in 4 different ways. First, we established an age-depth relationship based on the linear regression using the AMS ^{14}C dates at 45 and at 375 cm and by assuming a surface age of 0 cal. years BP (Fig.2b). According to this regression, we estimated an average sedimentation rate of 44.3 cm kyr^{-1}. In order to verify the validity of the age vs. depth relationship, we applied a second linear regression using the same data points without assuming an age of 0 cal yr BP at

the surface. The results showed an average sedimentation rate of 43.7 cm kyr^{-1} almost identical to our first estimation. Furthermore, we used the AMS ^{14}C dates at 38, 45, 71 and 375 cm in order to establish a linear regression by assuming a surface age of 0 cal. years BP. The calculated sedimentation rate was about 44.7 cm kyr^{-1}. Finally, we applied the linear regression through the 4 data points without assuming an age of 0 cal. years BP at the surface. The regression yielded an average sedimentation rate of 41.8 cm kyr^{-1}.

In conclusion, the variation in calculated ages possible for the age vs. depth relationships used for this core, is relatively small and we estimated the maximum variation at 6 % which does not affect the interpretation of our work. However, in the cases of omitting the surface age of 0 cal. years BP, we obtained an unrealistic age in the future at the top of the core. Thus the final age-depth relationship used for this core is based on the first assumption which considers a linear regression between a surface age of 0 cal. years BP and calibrated ^{14}C dates at 45 and 375 cm.

1.4.2. Geochemistry of organic matter in sediments

The geochemical and isotopic analyses of organic matter in the sediment show important variations in C_{org} content, C/N ratio, $\delta^{13}C_{org}$ and $\delta^{15}N$ values (Fig.3). The variations occurred simultaneously for all parameters and demonstrated two different trends in the upper and lower part of the analysed sequence. Hence, the sediment sequence can be divided in to two units: **Unit II** which extends from 176 to 100 cm (between ~ 4000 and ~ 2300 cal. years BP) and **Unit I** which covers the upper part of the sedimentary sequence (i.e. from 90 to 30 cm).

Unit II

The C_{org} content was relatively uniform throughout unit II and averaged 1.22%. The C_{org}/N ratio varied slightly between 10.2 and 10.9 and averaged 10.59 (Fig.3b). The $\delta^{13}C_{org}$ ranged from -23.5 and -22.95 ‰ (Fig.3c), whereas $\delta^{15}N$ values

remained close to 5.53 ‰ (Fig.3d). The values of C_{org}/N ratio, $\delta^{13}C_{org}$ and $\delta^{15}N$ are within the range commonly reported for marine organic matter (Meyers, 1994). This shows that marine productivity was the main source of organic matter, although the contribution of terrestrial input was significant (e.g., Muzuka and Hillaire Marcel, 1999).

Unit I

Higher values of C_{org} content characterized unit I. They increased up to 1.62% at 30 cm (Fig.3a). The trend of increasing values towards the top of the sequence may have resulted from enhanced flux of organic matter related to higher marine productivity (Meyers, 1994), as suggested by the decreasing C_{org}/N ratio values from 10.9 to 9.9 (Fig.3b) and the increasing δ^{13}Corg from -23.19 to -22.87‰. However, the increase in $\delta^{15}N$ values from 5.42 to 6.11‰ suggests increased continental inputs.

The transition between the two units occurred between 100 and 90 cm. This may represent a gradual transition but may also reflect smoothing due to bioturbation. The increase in C_{org} content at 100 cm corresponded to ~2300 cal. years BP.

1.4.3. Dinocyst assemblages

Dinocyst concentrations show large amplitude fluctuations over the last millennia but no clear trend. The density ranged between 10000 cysts g^{-1} and 33000 cysts g^{-1} and averaged 18271 cysts g^{-1}. A total of 14 dinocyst taxa were identified (Fig.4). Four taxa are heterotrophic (see Table 2). The dinocyst assemblages are dominated by cysts of *Pentapharsodinium dalei* and *Islandinium minutum*, which respectively averaged ~32% and ~28% of the assemblage. These two species are followed by *Operculodinium centrocarpum* (~19%) and *Nematosphaeropsis labyrinthus* (~10%), in addition to *Brigantedinium* spp. (~5%). The assemblages also include *Selenopemphix quanta, Islandinium? cezare*, *Spiniferites elongatus*, *Spiniferites ramosus, Spiniferites mirabilis-hyperacanthus*, *Spiniferites* spp.,

Ataxiodinium choane and the cysts of *Alexandrium tamarense*, which together accounted for less than 6%.

The variations in the composition of the assemblages were mostly driven by changes in the relative abundances of *Pentapharsodinium dalei*, which decreases from ~57 to ~11% relative to increase in *Operculodinium centrocarpum* (~10 to ~38%) and *Nematosphaeropsis labyrinthus* (~6 to ~18%). The fluctuations of the relative abundances of these taxa are difficult to interpret as they have a ubiquitous distribution in the northern North Atlantic and adjacent seas (Rochon *et al.*, 1999). Nevertheless, the increase of *Nematosphaeropsis labyrinthus* and *Spiniferites* spp., related to the decrease of *Pentapharsodinium dalei*, may reflect a trend toward warmer sea-surface conditions (Rochon *et al.*, 1999; de Vernal and Marret, 2007).

The other dominant taxon *Islandinium minutum*, and most of the secondary species showed high frequency oscillation but no clear trend. However, the relative abundances of the heterotrophic taxa *Brigantedinium* spp. and *Selenopemphix quanta* increased above 100 cm (~2300 cal. years BP) from ~0.7 to ~13% and from 0 to ~4%, respectively. This could be explained by changes in the trophic conditions reflecting increased productivity (e.g., de Vernal *et al.*, 2001; de Vernal and Marret, 2007; Radi and de Vernal, 2008).

1.4.4. Reconstructions of sea-surface conditions and pelagic productivity

The reconstructions show important variations in sea-surface temperature in summer (SST) and salinity (SSS) in summer in addition to sea-ice cover (Fig.5). Two different intervals can be distinguished. From 176 to 85 cm, the SST and SSS recorded high frequency oscillations of large amplitude (3.2 to 12.9°C and 29 to 32 respectively). The sea-ice cover also recorded large amplitude variations, from 3 to 6 months yr^{-1}. Between 105 and 85 cm, minimum SST and maximum sea-ice are recorded. This cold interval is centered around ~2100 cal. years BP. Above 85 cm, there was a trend of increasing SST from 6.3 to 12.4°C, concomitant with decreasing

sea-ice cover from 6 to 3 months yr^{-1}, and SSS that decreased up to 30. The upper part of the sequence, above 68 cm, recorded relatively stable conditions.

In order to reconstruct productivity, we used the modern analogue technique (Guiot and de Vernal, 2007) with reference to the MODIS database (http://daac.gsfc.nasa.gov). As shown by Radi and de Vernal (2008) such an approach permits reconstruction with an accuracy of ± 18%. The results suggest annual primary production of 250 gC m^{-2} yr^{-1} and show large amplitude oscillations with depth (Fig.5). In the lower part of the section, from 176 to 100 cm, the estimated productivity varied between 144 and 306 gC m^{-2} yr^{-1} and averaged 291gC m^{-2} yr^{-1}. Two minimum values were recorded in the interval between 100 and 88 cm; one at 94 cm (125 gC m^{-2} yr^{-1}) and the other at 90 cm (128 gC m^{-2} y^{-1}). In the upper part of the core, above 90 cm, the primary productivity reconstructions estimate particularly high values averaging 300 gC m^{-2} yr^{-1}. Therefore, the reconstructions suggest variations in productivity with a significant increase after ~ 1900 cal. years BP.

1.4.5. Benthic foraminiferal assemblages

Agglutinated benthic foraminifera are absent in the studied section of core COR503-37PC. However, the previous study of Genovesi (2009) reported their occurrence in the upper part of the box core COR503-37BC (0-5 cm). Their distribution and exclusive occurrence in surface sediment is likely due to poor preservation with increasing sediment depth (cf. Murray, 1991; Murray and Alve, 1999).

Calcareous benthic foraminifera were recorded in all samples. Their concentrations varied between 1.4 and 26.6 tests g^{-1} and averaged 7.2 tests g^{-1} (Fig.5). The abundance remained relatively low ($\leq$ 7 tests g^{-1}) in the lower part of the section, especially below 104 cm. They were slightly higher in the upper part of the core and varied between 3 and 26.6 tests g^{-1}.

Of the 21 identified benthic calcareous foraminiferal species (see Table 3), 4 dominate the assemblages. The dominant species include *Bulimina marginata*,

Bulimina exilis, *Elphidium excavatum* and *Nonionellina labradorica*. The secondary species are *Brizalina subaenariensis*, *Buccella frigida*, *Glandulina laevigata*, *Globobulimina auriculata*, *Lagena* sp. and *Islandiella norcrossi*. The remaining species that were occasionally present are *Bolivina inflata*, *Cassidulina reniforme*, *Cibicides lobatulus*, *Cibicides pseudoungerianus*, *Dentalina* sp., *Fissurina* sp., *Lenticulina* sp., *Nonionellina turgida*, *Oolina hexagona*, *Oridorsalis umbonatus* and *Quinqueloculina seminulum*.

Major changes characterized the benthic foraminiferal assemblages, which led to distinguish three assemblages with different patterns throughout the core. The first one was recorded between 176 and 128 cm (i.e. 4000 - 2900 years BP) and is characterized by the dominance of *B. exilis* followed by *B. marginata* which averaged 49% and 28%, respectively. The relative abundance of *N. labradorica* and *E. excavatum* was relatively low (averaged 3 and 7%, respectively) and started increasing slightly at the top of the interval. The relative abundances of *G. auriculata* and *I. norcrossi* remained low throughout the sequence.

The second assemblage, between 128 and 88 cm (2900 – 2000 cal. year BP), was characterized by the disappearance of *B. subaenariensis*, *G. laevigata* and *Q. seminulum* and the appearance of *G. auriculata* and *I. norcrossi*. The maximum relative abundances of *N. labradorica* and *E. excavatum* was recorded at the beginning of this interval (up to 37% and 39%, respectively). This interval was also characterised by the decrease of the relative abundance of *B. exilis* from 49 to 28%. This could be explained by the decrease of the fresh and unaltered organic matter input (Jorissen *et al.*, 2007).

The upper assemblage, recorded from 88 to 30 cm, was characterised by the appearance of *B. frigida* and the reappearance of *G.laevigata*, *Q. seminulum* and *B. subaenariensis*, which recorded a peak at 70 cm then decreased towards the top of the zone. The percentage of *N. labradorica* increased to 14% in the upper part of the sequence. The increase in the relative abundance of *B. subaenariensis*, *G. auriculata*, *B. exilis* and *B. marginata* indicates changes in the hydrographical conditions of the

bottom water at the GSL during the last centuries. This trend suggest also a decrease in the dissolved oxygen concentrations, as these taxa are reported from low level oxygen environments (Sen Gupta Machain-Castillo, 1993; Fontanier *et al.*, 2002; Murray, 2001; Jorissen *et al.*, 2007).

1.4.6. Isotopic composition of benthic foraminiferal shells

As mentioned in the method section, isotopic analyses were performed on two species of benthic foraminifers, *Bulimina exilis* and *Bulimina marginata*, in order to verify if we could develop a multispecies record. The results (Fig.7) show that the $\delta^{18}O$ of *B. marginata* was slightly depleted relative to *B. exilis*. However, the values can be comparable when taking into account the analytical reproducibility, and the fact that the two species do not occupy exactly the same depth in the sediment. The $\delta^{13}C$ results, on the other hand, strongly differed. *B. exilis* had values significantly lower (~2 ‰) relative to *B. marginata*. This could be explained by the fact that *B. marginata* is a shallow infaunal species living close to the sediment-water interface whereas *B. exilis* is a deep infaunal species (Jorissen, 1999; Jorissen *et al.*, 1998). Thus, the $\delta^{13}C$ of *B. exilis* reflects the depletion of $\delta^{13}C$ pore waters after oxidation of organic matter in the sediment (e.g., Corliss, 1985). Here, we chose to analyse *B. marginata* since it better reflects the isotopic composition of bottom waters.

The difference in the $\delta^{13}C$ values between the two species is also enhanced by the comparison of the results obtained from *B. marginata* in the upper part of the piston core (this study) and from *B. exilis* in the box core COR503-37BC (Genovesi, 2009) (Fig.8). The results show similar $\delta^{18}O$ values for both species but very different $\delta^{13}C$ values. *B. marginata* values ranged between -0.32 to 0.25 ‰, which is notably heavier than those of *B. exilis*, which ranged between -2.37 ‰ and -1.63 ‰.

In core COR503-37PC, the $\delta^{13}C$ values of *B. marginata* showed little variation. Nevertheless, a slight diminution of $\delta^{13}C$ values from 0.06 ± 0.05 ‰ to -0.32 ± 0.05 ‰, seems to characterize the upper part of the core (above 60 cm).

The $\delta^{18}O$ profile of *B. marginata* shows variations ranging from 2.08 to 3.09‰. A decrease from ~2.75 ‰ to ~2.58 ‰ was recorded from the base of the section to 132 cm. In the upper part of the core, $\delta^{18}O$ values increased from ~ 2.56 to 2.91 ‰ between 112 and 64 cm (i.e. from ~2500 to ~1500years BP) and decreased to ~ 2.57 ‰ at the top of the sedimentary sequence. Such variations are significant and may reflect changes in the isotopic composition of sea-water or changes in temperature.

If we make the assumption of quasi-uniform $\delta^{18}O$ of sea water (cf. Thibodeau *et al.*, 2010; Genovesi *et al.*, submitted.) we can estimate the bottom water temperature by applying the paleotemperature equation of Skackleton (1974) to the $\delta^{18}O$ data from *B marginata*. The equation is as follows:

$$t = 16.9 - 4.38*(\delta^{18}O_c - \delta^{18}O_w + 0.27) + 0.10*(\delta^{18}O_c - \delta^{18}O_w + 0.27)^2$$

where t represents the temperature (in °C) of the ambient water in which calcite is precipitated, $\delta^{18}O_c$ is the isotopic composition of the calcite (measured in *B. marginata*) (versus V-PDB), $\delta^{18}O_w$ is the isotopic composition of the ambient water (versus V-SMOW). For the $\delta^{18}O_w$, we used a value of 0.07‰ as did Genovesi (2009). This value corresponds to an average of $\delta^{18}O$ measurements in the Gulf of St. Lawrence collected between 350 and 450 m (cf. Schmidt *et al.*, 1999).

The estimation of temperature indicates important variation in the properties of the deep water in the Laurentian Channel. The temperature estimation ranged from 2°C to 7°C, with an average temperature of ± 4.8°C (Fig.9a). According to $\delta^{18}O$ data, the temperature corresponds to present day values. Minimum temperatures were recorded between 112 and 84 cm, which corresponds to ~ 2500-1900 cal. years BP. The top of the record is marked by a trend toward higher values and therefore warmer conditions.

1.5. Discussion

1.5.1. Pelagic productivity and organic carbon flux

The C_{org} and C_{org}/N contents in the upper 10 cm (i.e. 30-40 cm) of COR503-37PC averaged 1.6 % and 9.9 respectively. Such values are higher than what was measured in core COR503-37BC (average C_{org} of 1 % and C/N of 6.3; cf. Genovesi, 2009), yet, they are within the lower range of those recorded in the Laurentian Channel (Muzuka and Hillaire Marcel, 1999) and in Cabot Strait (Mucci *et al.*, 2000). The difference in C_{org} content in the two data sets could result from the use of two different analytical methods to determine the bulk C_{org} concentrations in the sediment. For this study, we used the fumigation method (Hélie, 2005), whereas Genovesi (2009) used an acidification technique, which is a method that can lead to underestimation of the C_{org} content due to imperfect dissolution of non organic remains (Hélie, 2005). In order to verify this assumption, several tests were made using aliquots of both cores. Results confirm the systematic difference between the two approaches, with fumigation yielding higher organic carbon values and more reliable data.

The C_{org} content in the core ranged from 1.15 to 1.6%, and between 176 and 106 cm values were relatively uniform at 1.2 ± 0.1%. The C_{org} content had a sharp increase from 1.2 to 1.45% at about 100 cm. In the upper part of the core, C_{org} values increased gradually to reach up to 1.62% at 30 cm. The increase in the relative organic content in the sediment occurred at ~2300 cal. years BP. It could have resulted from higher organic fluxes or lesser dilution with inorganic particles. In the latter case, it could be related to increased marine productivity or to increased terrestrial organic matter input (Meyers, 1994). Alternatively, the higher organic carbon in the upper part of the core could be due to better preservation of organic matter, notably because of low dissolved oxygen levels (Meyers, 1994).

The marked change in organic carbon content at ~2300 years BP was accompanied by changes in the C_{org}/N ratio and $\delta^{13}C_{org}$, which suggests an increase in the marine inputs relative to terrestrial organic matter (e.g., Muzuka and Hillaire Marcel, 1999). Therefore, both the C_{org}/N ratio and the isotopic composition of organic carbon suggest increased organic carbon fluxes of marine origin during the last two millennia.

In contrast, $\delta^{15}N$ follows an opposite trend and drifts slightly towards higher values to reach values recorded in COR503-37BC. This could be explained by the increase in terrestrial organic matter (Montoya, 1994), but appears unlikely if we rely on the C_{org}/N ratio and $\delta^{13}C_{org}$ values. Alternatively, the trend could result from an increase in nitrate uptake by changing phytoplanktonic populations (e.g., Muzuka and Hillaire Marcel, 1999; McKay, 2004) as observed in the Southern Ocean, where higher $\delta^{15}N$ values indicated high efficiency and utilization rate of surface nitrate by phytoplankton (François *et al.*, 1994).

Independently from the geochemical and isotopic data, the palynological record suggests an important change in the pelagic productivity since ~ 2300 cal. years BP, which is probably related to a change in the hydrography that is marked by lower salinities suggesting enhanced freshwater input and more estuarine conditions. The dinocyst concentrations remained high throughout the sequence (averaged ~20000 cyst g^{-1}), but important changes in dinocyst assemblages were observed with a significant increase in the proportion of the heterotrophic taxa *Brigantedinium* spp. and *Selenopemphix quanta*. Such a transition reflects changes in trophic conditions and increase in productivity (e.g., de Vernal *et al.*, 2001; de Vernal and Marret 2007, Radi and de Vernal, 2008). The reconstruction of sea-surface conditions indicate warmer SSTs during the last 1500 years, as suggested by the increase of *Nematosphaeropsis labyrinthus* and *Spiniferites* spp. and the decrease of *Pentapharsodinium dalei*. The reconstruction of the annual primary production based on the dinocyst assemblages suggests variations from 120 to 320 gC $m^{-2}yr^{-1}$ with

significantly higher values in the upper part of the core, above 90 cm which corresponds to the last 2000 years. The reconstructed primary productivity between 60 and 30 cm averaged 302 ± 54 gC $m^{-2}yr^{-1}$, which is consistent with estimates from the analyses of the box core that spans the last two centuries (Genovesi 2009; Genovesi *et al.*, submitted).

1.5.2. Bottom water conditions

The abundance and distribution of benthic foraminifera can be controlled by changes in physical and chemical parameters such as temperature, salinity, dissolved oxygen concentration, light and turbidity (Murray, 1991; 2001). Many studies used foraminifera as indicators of hypoxic water (e.g., Osterman, 2003; Osterman *et al.*, 2009; Kaiho; 1994) and changes in productivity (e.g., Mojtahid *et al.*, 2008). Therefore, the variation observed in the benthic foraminiferal assemblages can reflect significant changes in environmental and oceanographic conditions in the GSL during the last millennia. The analysis of core COR503-37PC reveals an increase of the benthic foraminiferal concentrations toward the surface, which roughly corresponds with the increase in pelagic productivity and higher C_{org} content. The higher concentration of benthic foraminifera could be a response to the higher fluxes of organic matter (Leckie and Olson, 2003). That is also confirmed by the dominance of *B. exilis,* a benthic foraminifer generally associated with high organic matter inputs (Jorissen *et al.*, 2007). The increase of the relative abundances of *B. subaenariensis* and *G. auriculata* in the upper part of the sedimentary sequence may also be an indication of a decrease in the dissolved oxygen (Sen Gupta and Machain-Castillo, 1993; Murray, 2001; Jorissen *et al.*, 2007). Moreover, the variations of the relative abundances of *N. labradorica*, which is a characteristic species of the Labrador Sea (Bilodeau *et al.*, 1994), can reflect the changes in the contribution of the LCW relative to NACW in the bottom water of the GSL. In the study carried out by Genovesi *et al.* (submitted), the recent decrease in the relative abundance of *N.*

labradorica matches the increase in bottom water temperature as estimated from $\delta^{18}O$ in foraminiferal tests. This recent trend has been associated with the decrease in the contribution of the cold and highly oxygenated LCW as observed since the 1930s (cf. Gilbert *et al.*, 2005). In our study, we noted variations of the abundance *N. labradorica* but the relationship with the estimated temperature based on $\delta^{18}O$ are not unequivocal.

The maximum of *N. labradorica* between 120 and 90 cm would suggest a maximum contribution of LWC at ~2700- 2000 cal. years BP, whereas the upper part of the core marked by the co-occurrence of *B. subaenariensis*, *B. frigida* and *Globobulimina auriculata* shows estuarine characteristics (Jorissen *et al.*, 2007)

The $\delta^{18}O$ in benthic foraminifera provides additional information on bottom water properties. Although difficult to interpret precisely without data on the isotopic composition of bottom waters, the $\delta^{18}O$ signal shows millennial scale oscillations (Fig.9a).

The benthic foraminiferal assemblages and their isotopic composition, therefore, illustrate changes in the properties of bottom waters that are related to several parameters, which likely include temperature, sea-surface conditions, pelagic productivity and biogenic fluxes to the sea-floor and oxygen concentration.

1.6. Conclusion

Micropaleontological, geochemical and isotopic analyses of sediments from core COR0503-CL05-37PC collected in the Laurentian Channel in the central part of the Gulf of St. Lawrence show important environmental changes over the last millennia. These changes are related to variation in the biogenic productivity in the upper water mass and subsequent flux of organic matter. They are also related to variations in bottom water temperatures. These parameters are however decoupled in our records. The data suggest a major change in productivity and organic fluxes after

~2300 years BP, whereas the estimated bottom water temperatures suggest millennial oscillations with colder conditions being recorded prior to 2800 cal. years BP and at ~1800 cal. years BP.

The variations recorded here differ from those documented during recent centuries in the St. Lawrence Estuary (Thibodeau *et al.;* 2006, 2010) and in the Gulf of St. Lawrence (Genovesi, 2009; Genovesi *et al.*, submitted). In the Estuary, there has been a recent decrease in bottom water oxygen content corresponding to both increased productivity, organic fluxes (Thibodeau *et al.*, 2006) and warming in bottom waters since the turn of the last century (Thibodeau *et al.*, 2010). In the Gulf, where there is high productivity with no significant changes at the scale of the last centuries, the trend towards hypoxia seems rather related to warming of bottom waters (Genovesi *et al.*, submitted). Our data that extend back in time, much prior to the period of human occupation, show complex variations of productivity and bottom water conditions that are related to natural variations. They illustrate forcing at millennial scales to which centennial variations such as those observed by Thibodeau *et al.* (2006; 2010) and (Genovesi, 2009) are superimposed. They demonstrate the sensitivity of the St. Lawrence Estuary and Gulf ecosystems. The data also suggest that the general conditions that prevail since in the last few centuries in the Gulf of St. Lawrence, with relatively warm bottom temperature and high pelagic productivity, lead to enhanced sensitivity of the system towards hypoxia.

1.7. References

Barletta, F., St-onge, G., Stoner, J.S., and Lajeunesse, P., 2010. A high-resolution Holocene paleomagnetic secular variation and relative paleointensity stack from eastern Canada, Earth Planet. Sci. Lett. (2010), doi:10.1016/j.epsl.2010.07.038

Benoit, P., Gratton, Y., and Mucci, A., 2006. Modeling of dissolved oxygen levels in the bottom waters of the Lower St. Lawrence Estuary: coupling of benthic and pelagic processes. Marine Chemistry 102, 13-32.

Berhenfeld, M.J., and Falkowski, P.G., 1997. Photosynthetic rates derived from satellite based chlorophyll concentration. Limnol. Oceanogr. 42, 1-20.

Bilodeau, G., de Vernal, A., and Hillaire-Marcel, C., 1994. Benthic foraminiferal assemblages in Labrador Sea sediments: relations with deep-water mass changes since deglaciation. Can. J. Earth. Sci. 31, 128-138.

Bratton, J.F., Colman, S.M., and Seal II, R.R., 2003. Eutrophication and carbon sources in Chesapeake Bay over the last 2700 yr: Human impact in context. Geochim. Cosmochim. Acta. 67, 3385–3402.

Bugden, G.L., 1991. Changes in temperature-salinity characteristics of the deep waters of the Gulf of St. Lawrence over the past several decades. In Therriault. J.C., The Gulf of St. Lawrence: Small Ocean or a big estuary? Can.Spec.Publ.Fish.Aquat.Sci.13, 139-174.

Chabot, D., and Dutil, J.D., 1999. Reduced growth of Atlantic cod in non-lethal hypoxic conditions. J. Fish Biology, 55, 472-491.

Cloern, J.E., 2001. Our evolving conceptual model of the coastal eutrophication problem. Mar. Ecol. Prog. Ser. 210, 223-253.

Coplen, T.B., 1995. Discontinuance of SMOW and Pdb. Nature. 375, 285.

Corliss, B.H.,1985. Microhabit of benthic foraminifera within deep-sea sediments. Nature,314,151-438.

Craig, J.K., Crowder, L.B., Gray, C.D., McDaniel, C.J., Henwood, T.A., and Hanifen, J.G., 2001. Ecological effects of hypoxia on fish, sea turtles, and marine mammals in the northwestern Gulf of Mexico. *In.* Costal Hypoxia: consequences for living resources and ecosystems. Coastal and Estuarine Studies 58. American Geophysical Union, Washington D.C, 269-292.

de Vernal, A., Guiot, J., and Turon, J.L., 1993. Late and postglacial paleoenvironments of the Gulf of St. Lawrence: Marine and terrestrial palynological evidence. Géographie physique et Quaternaire 42 (2), 167-180.
de Vernal, A., Henry, M., and Bilodeau, G., 1996. Techniques de préparation et d'analyse en micropaléontologie. Les cahiers du GEOTOP. Unpublished report. http://gizmo.geotop.uqam.ca//Gestion_Documents/Cahiers/Micropaleontologie_cahier3.pdf

de Vernal, A., Rochon, A., Turon, J.-L., and Matthiessen, J., 1997. Organic-walled dinoflagellate cysts: palynological tracers of seasurface conditions in middle to high latitude marine environments. Geobios, 30, 905–920.

de Vernal, A., Henry, M., Matthiessen, J., Mudie, P.J., Rochon, A., Boessenkool, K.P., Eynaud, F., Grosfjeld, K., Guiot, J. and Hamel, D., 2001. Dinoflagellate cyst assemblages as tracers of sea-surface conditions in the northern North Atlantic, Arctic and sub-Arctic seas: the new" n= 677" data base and its application for quantitative paleoceanographic reconstruction. Journal of Quaternary Science, 16(7), 681-698.

de Vernal, A., Eynauld, F., Henry, M., Hillaire-Marcel, C., Londeix, L., Mangin, S., Matthiessen, J., Marret, F., Radi, T., Rochon, A., Solignac, S., and Turon, J.L., 2005. Reconstruction of sea-surface conditions at middle to high latitudes of the Northern Hemisphere during the Last Glacial Maximum (LGM) based on dinoflagellate cyst assemblages. Quaternary Science Reviews. 24, 897–924.

de Vernal, A., and Marret, F., 2007. Organic-Walled Dinoflagellate Cysts:Tracers of Sea-Surface Conditions. *In,* Hillaire-Marcel, C., and de Vernal, A., (Ed). 2007. Developments in marine geology Volume1: Proxies in late Cenozoic paleoceanography, GEOTOP. Université du Québec à Montréal, Québec, Chapter9, 371-408.

den Dulk, M.., Reichart, G.J., van Heyst, S., Zachariasse, W.J., and Vaen der Zwaan, G.J., 2000. Benthic foraminifera as proxies of organic matter flux and bottom water oxygenation? A case history from the northern Arabian Sea. Palaeogeography, Palaeoclimatology, Palaeoecology, 161,337–359.

Dhahri, N., 2010. Variabilité naturelle des conditions pélagiques et benthiques dans le golfe du Saint-Laurent à l'Holocène supérieur. Msc. Thesis. Université du Québec à Montréal, 84pp.

Diaz, R., and Rosenberg, R., 1995. Marine benthic hypoxia: a review of its ecological effects and the behaviour responses of benthic macrofauna.Oceanogr. Mar. Biol. Annu, Rev, 33, 245-303.

Diaz, R., and Rosenberg, R., 2008. Spreading dead zones and consequences for marine ecosystems. Science, 321, 926-929.

Dickie, L., and Trites, L.M. 1983. The Gulf of St. Lawrence. *In* Estuaries and enclosed seas. (Ed) B.H. Ketchum. Elsevier, Amsterdam, The Netherlands. pp, 403–425.

El Sabh, M., 1973. Seasonal and long term variations of the water properties in the Gulf of St. Lawrence . *In* El Sabh, M., [ed]. Proc. Workshop Physical sciences in the Gulf of St. Lawrence. pp, 128-158.

Fontanier, C., Jorissen, F.J., Licari, L., Alexandre, A., Anschutz, P., and Carbonel, P., 2002. Live benthic foraminiferal faunas from the Bay of Biscay: faunal density, composition, and microhabitats. Deep-Sea Research I 49, 751–785.

François, R., Altabet, M.A., Yu, E.F., Sigman, D.M., Bacon, M.P., Frank, M., Bohrmann, G., Bareille, G., and Labeyrie, L.D., 1997. Contribution of Southern Ocean surface-water stratification to low atmospheric CO_2 concentrations during the last glacial period. Nature, 389, 929-935.

Genovesi, L., 2009. Indices micropaléontologiques et géochimiques de changements récents de l'oxygénation et la température des eaux profondes du Golfe du ST-Laurent. Msc. Thesis. Université du Québec à Montréal, 71pp.

Genovesi, L., de Vernal, A., Thibodeau, B., Hillaire-Marcel, C., Mucci, A., and Gilbert, D., *submitted.* Recent changes in bottom water oxygenation and temperature in the Gulf of St. Lawrence: micropaleontological and geochemical evidence.

Gilbert, D., and Pettigrew, B., 1997. Inetrannual variability the CIL core temperature in the Gulf of St. Lawrence. Can. J. Fish. Aquat. Sci. 54 (1), 57-67.

Gilbert, D., Sundby, B., Gobeil, C., Mucci, A,. and Tremblay, G-H., 2005. A seventy-two-year record of diminishing deep water oxygen in the St Lawrence estuary: The Northwest Atlantic connection. Limnol. Oceanogr. 50, 1654-1666.

Gilbert, D., Chabot, D., Archambaut, P., Rondeau, B., and Herbert, S., 2007. Appauvrissement en oxygène dissous dans les eaux profondes du Saint-Laurent marin : Causes possibles et impacts écologiques. Le Naturaliste Canadien, 131 (1), 67-75.

Gilbert, D., Rabalais, N.N., Diaz, R.J., and Zhang, J., 2010. Evidence for greater oxygen decline rates in the coastal ocean than in the open ocean. Biogeosciences, 7, 2283-2296.

Guiot, J., and de Vernal, A., 2007. Transfert functions: methods for quantitative paeleoceanography based on microfossils. *In,* Hillaire-Marcel, C., and de Vernal, A., (Ed). 2007. Developments in marine geology Volume1: Proxies in late Cenozoic paleoceanography, GEOTOP. Université du Québec à Montréal, Québec, Chapter 13, 523-563.

Hélie, J.F., 2009. Elemental and stable isotopic approaches for studying the organic and inorganic carbon components in natural samples. From Deep-Sea to Coastal Zones: Methods – Techniques for Studying Paleoenvironments, IOP Conference Series: Earth and Environmental Science, 5, 012005, doi:10.1088/1755-1307/5/1/012005

Hughen, K. A., Baillie, M.G.L., Bard, E., Bayliss, A., Beck, J.W., Blackwell, P.G., Buck, C.E., Burr, G.S., Cutler, K.B., Damon, P.E., Edwards, R.L., Fairbanks, R.G., Friedrich, M., Guilderson, T.P., Herring, C., Kromer, B., McCormac, F.G., Manning, S.W., Ramsey, C.B., Reimer, P.J., Reimer, R.W., Remmele, S., Southon, J.R., Stuiver, M., Talamo, S., Taylor, F.W., van der Plicht, J., and Weyhenmeyer, C.E. 2004. Marine04 Marine radiocarbon age calibration, 26 - 0 ka BP. Radiocarbon 46, 1059-1086.

Jorissen, F.J., Wittling, I., Peypouquet, J.P., Rabouille, C., and Relexans, J.C., 1998. Live benthic foraminiferal faunas off Cape Blanc, NW Africa; Community structure and microhabitats. Deep-Sea Res., I 45, 2157-2188.

Jorissen, F.J, 1999. Benthic foraminiferal successions across Late Quaternary Mediterranean sapropels. Marine Geology 153, 91–101.

Jorissen, F.J, Fontanier, C., and Thomas, E., 2007. Paleoceanographical proxies based on deep-sea Benthic foraminiferal assemblage characteristics. *In,* Hillaire-Marcel, C., and de Vernal, A., (Ed). 2007. Developments in marine geology Volume1: Proxies in late Cenozoic paleoceanography, GEOTOP. Université du Québec à Montréal, Québec, Chapter 7, 263-325.

Kaiho, K., 1994. Benthic foraminiferal dissolved-oxygen index and dissolved-oxygen levels in the modern ocean. Geology 22, 719-722.

Keeling, R.F., and Garcia, H.E., 2002. The change in Oceanic O_2 inventory associated with recent global warming, P.Natl.Acad.Sci. USA, 99 (12),7848-7853: doi: 10.1073/pnas.122154899.

Leckie, R.M., and Olson, H.C., 2003. Foraminifera as proxies for sea-level Change on siliciclastic margins. Micropaleontologic proxies for seal-level Change and stratigraphic Discontinuities. SPEM. 75, 5-19.

Loring, D.H., and Nota, D.J.G., 1973. Morphology and sediments of the Gulf of St.Lawrence. Bull. Fish. Res. Bd Can.182, pp147.

Matthews, J., 1969. The assessment of a method for the determination of absolute pollen frequencies. New Phytologist68 (1), 161-166.

McKay, J.L., Pedersen, T.F., and Kienast, S.S., 2004. Organic carbon accumulation over the last 16 kyr off Vancouver Island, Canada: evidence for increased marine productivity during the deglacial. Quaternary Science Reviews, 23, 261–281.

Meyers, P.A., 1994. Preservation of elemental and isotopic source identification of sedimentary organic matter. Chem.Geol, 114, 289-302.

Meyers, P.A, 1997. Organic geochemical proxies of paleoceanographic, paleolimnologic, and paleoclimatic processes. Org. Geochem. 27, N^0 5/6, 213-250.

Mojtahid. M., Jorissen, F., and Person, T.H., 2008. Comparison of benthic foraminiferal and macrofaunal responses to organic pollution in the Firth of Clyde (Scotland). Marine Pollution Bulletin, 56, 42–76.

Montoya, J.P., 1994. Nitrogen isotope fractionation in the modern ocean: implications for the sedimentary record. *In*: Zahn, R., Pedersen, T.F., Kaminski, M.A., Labeyrie, L. (Eds.), Carbon Cycling in the Glacial Ocean: Constraints on the Ocean's Role in Global Change. NATO ASI Series, Vol. 117. Springer, Berlin, pp 259–279.

Mucci, A., Sundby, B., Gehlen, M., Arakaki, T., Zhong, S., and Silverberg, N., 2000.The fate of carbon in continental shelf sediments of eastern Canada: a case study. Deep-sea Research II (47), 733-760.

Murray, J.W., and Alve, E., 1999. Taphonomic experiments on marginal marine foraminiferal assemblages: how much ecological information is preserved? Palaeogeography, Palaeoclimatology, Palaeoecology ,149, 183–197.

Murray, J.W., 2001. The niche of benthic foraminifera, critical thresholds and proxies. Marine Micropaleontology, 41, 1-7.

Muzuka, A.N.N., and Hillaire-Marcel, C. 1999. Burial rates of organic matter along the eastern Canadian margin and stable isotope constraints on its origin and diagenetic evolution. Mar. Geol., 160, 251-27.

Osterman, L.E., 2003. Benthic foraminifers from the continental shelf and slope of the Gulf of Mexico: an indicator of shelf hypoxia. Estuarine, Coastal and Shelf Science, 58, 17–35.

Osterman, L.E., Poore, R.Z., Swarzenski, P.W., Senn, D.B., and DiMarco, S.F., 2009. The 20th-century development and expansion of Louisiana shelf hypoxia, Gulf of Mexico. Geo-Mar. Lett., 29, 405–414.

Radi, T., Pospelova, V., de Vernal, A., and Barrie, J.V., 2007. Dinoflagellate cysts as indicators of water quality and productivity in British Columbia estuarine environments. Marine Micropaleontology, 62, 269-297.

Radi, T., and de Vernal, A., 2008. Dinocysts as proxy of primary productivity in mid-high latitudes of the Northen Hemisphere. Marine Micropaleontology, 68, 84-114.

Ravelo, A., and Hillaire-Marcel, C., 2007. The use of Oxygen and Carbon isotopes of foraminifera in paleoceanography. *In*, Hillaire-Marcel, C., and de Vernal, A., (Ed). 2007. Developments in marine geology Volume1: Proxies in late Cenozoic paleoceanography, GEOTOP. Université du Québec à Montréal, Québec, Chapter18,735-764.

Rochon, A., de Vernal, A., Turon, J.L., Matthiessen, J., and Head, M.J., 1999. Distribution of recent dinoflagellate cysts in surface sediments from the North Atlantic ocean and adjacent seas inrelation to sea-surface parameters. Am. Assoc. Stratigr. Palynol. Found. 35. 152pp.

Rodrigues, C.G., 1980. Holocene microfauna and paleoceanography of the Gulf of St. Lawrence. Ph.D. Thesis. Carleton University.

Saucier, F.J., Roy, F., Gilbert, D., Pellerin, P., and Ritchie, H., 2003. The formation and circulation process of water masses in the Gulf of St.Lawrence. J.Geo.Res.108, 3269-3289.

Savenkoff, C., Vézina, A.F., Packard, T.T., Silverbeg, N., Therriault, J.C., Chen, W., Bérubé, C., Mucci, A., Klein, B., Mesplé, F., Tremblay, J.E., Legendre, L., Wesson, J., and Ingram, R.G., 1996. Distributions of oxygen, carbon, and respiratory activity in the deep layer of the Gulf of St. Lawrence and their implications for the carbon cycle. Can. J. Fish. Aquat. Sci., 53, 2451–2465.

Schmidt, G.A., Bigg, G. R., and Rohling, E. J. 1999. Global Seawater Oxygen-18 Database. http://data.giss.nasa.gov/o18data/

Sen Gupta, B.K., and Machain-Castillo, M.L., 1993. Benthic foraminifera in oxygen-poor-habitats.Marine Micropaleontology, 20, 183-201.

Shackleton, N.J., 1974. Attainment of isotopic equilibrium between ocean water and the benthonic foraminifera genus Uvigerina: isotopic changes in the ocean during the last glacial. *In* J. Labeyrie [ed], Méthodes quantitatives d'études des variations du climat au cours du Pléistocène, Éditions du CNRS. p.203-209.

Stuiver, M., Reimer, P.J., and Reimer, R.W., 2005. CALIB 5.0. Available from http://calib.qub.ac.uk/calib/

Thibodeau, B., de Vernal, A., and Mucci, A., 2006. Recent eutrophication and consequent hypoxia in the bottom waters of the Lower St. Lawrence Estuary: Micropaleontological and geochemical evidence. Marine Geology, 231, 37-50.

Thibodeau, B., de Vernal, A., Hillaire-Marcel, C., and Mucci, A., ***In Press***. 20th Century warming in deep waters of the Gulf of St. Lawrence: a unique feature of the last millennium, *Geophysical Research Letters*.

Verity, P.G., Alber, M., and Bricker, S.B., 2006. Development of hypoxia in well-mixed subtropical estuaries in the southeastern USA. Estuary. Coasts 29, 665–673.

Waelbroeck, C., Labeyrie, L., Michel, E., Duplessy, J.C., Mc Manus, J.F., Lambeck, K., Balbon, E., and Labracherie, M., 2002. Sea-level and deep water temperature changes derived from benthic foraminifera isotopic records. Quaternary Science Reviews, 21, 295-305.

Wu, R.S.S., 2002. Hypoxia: from molecular responses to ecosystem responses. Marine Pollution Bulletin, 45, 35-45.

Table 1: Radiocarbon dates in core COR503-37PC

Depth (cm)	Dated Materiel	Uncorrected Age AMS - ^{14}C Age (years BP)	Calibrated Age Interval (1σ) (years BP)	Study	Laboratory	Laboratory number
38	Shell fragments	620 ± 15	234-308 (271)	Barletta *et al.*, (2010)	Keck Carbon Cycle AMS Facility (University of California)	UCIAMS-40619
45	Shell fragments	1380 ± 35	890-966 (928)	This study	Lawrence Livermore National Laboratory	146824
71	Shell fragments	1525 ± 15	1004-1153 (1079)	Barletta *et al.*, (2010)	Keck Carbon Cycle AMS Facility (University of California)	UCIAMS-40623
375	Shell fragments	8030 ± 25	8406-8557 (8482)	Barletta *et al.*, (in press)	Keck Carbon Cycle AMS Facility (University of California)	UCIAMS-40621
474	Shell fragments	8555 ± 25	9086-9300 (9193)	Barletta *et al.*, (2010)	Keck Carbon Cycle AMS Facility (University of California)	UCIAMS-40618
657	Shell fragments	9160 ± 20	9845-10108 (9977)	Barletta *et al.*, (2010)	Keck Carbon Cycle AMS Facility (University of California)	UCIAMS-40615

Table 2: List of dinocyst taxa recorded in core COR503-37PC

Autotrophic taxa
Alexandrium tamarense type cyst
Ataxiodinium choane
Cyst of *Pentapharsodinium dalei*
Nematosphaeropsis labyrinthus
Operculodinium centrocarpum short processes
Operculodinium centrocarpum
Spiniferites elongatus
Spiniferites mirabilis-hyperacanthus
Spiniferites ramosus
Spiniferites spp.
Heterotrophic taxa
Brigantedinium spp.
Islandinium minutum
Islandinium? cezare
Selenopemphix quanta

Table 3: List of benthic foraminifer species recorded in core COR503-37PC

Bolivina inflata (Heron-Allen and Earland, 1913)
Brizalina subaenariensis (Cushman, 1922)
Buccella frigida (Cushman, 1922)
Bulimina exilis (Whitelegge, 1907)
Bulimina marginata (d'Orbigny 1826)
Cassidulina reniforme (Nørvang, 1945)
Cibicides lobatulus (Walker and Jacob 1798)
Cibicides pseudoungerianus (Cushman, 1922)
Dentalina sp.
Elphidium excavatum (Terquem 1876)
Fissurina sp.
Glandulina laevigata (d'Orbigny 1846)
Globobulimina auriculata (Bailey, 1851)
Islandiella norcrossi (Cushman, 1933)
Lagena sp.
Lenticulina sp.
Nonionellina labradorica (Dawson, 1860)
Nonionellina turgida (Williamson, 1958)
Oolina hexagona (Williamson, 1848)
Oridorsalis umbonatus (Reuss, 1851)
Quinqueloculina seminulum (Linné, 1758)

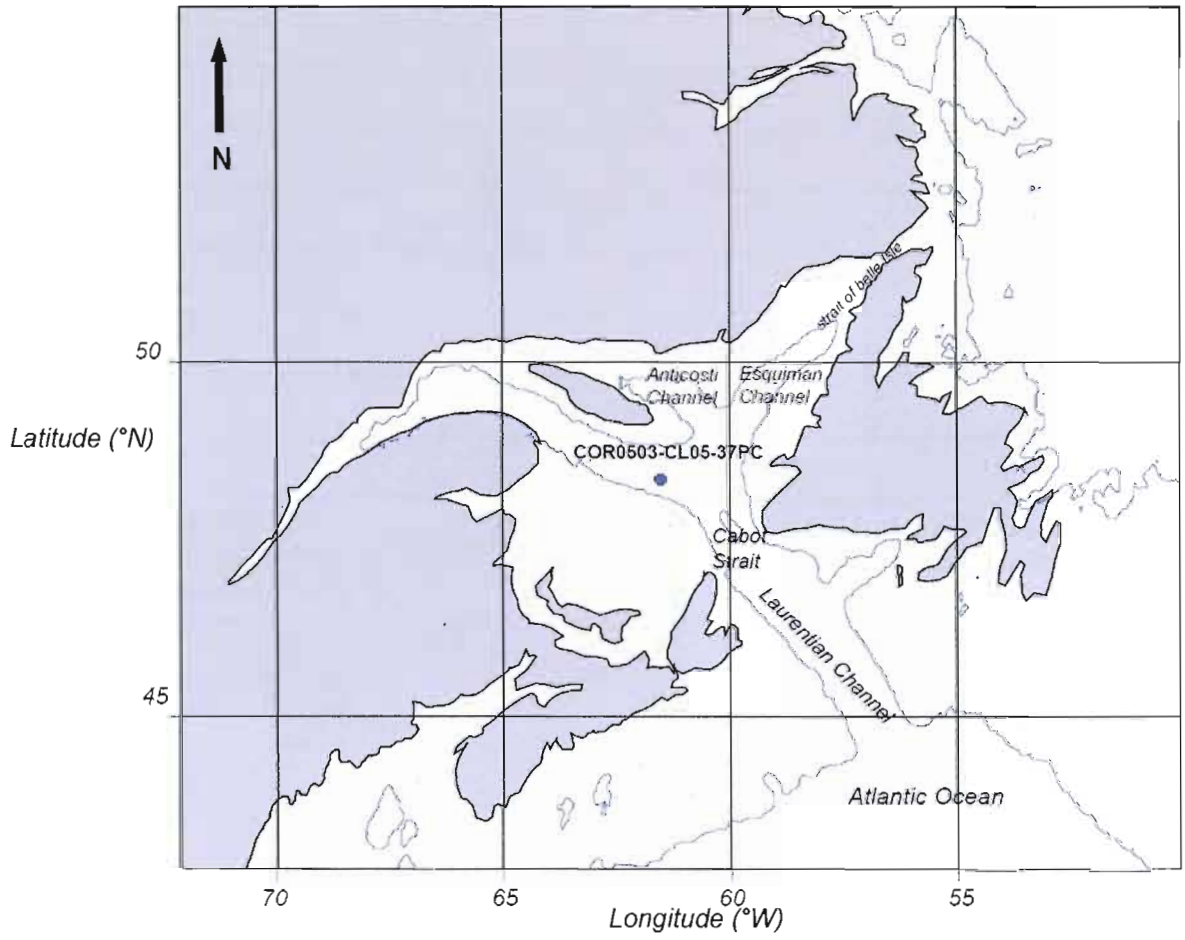

Figure 1: Map of the Gulf of St. Lawrence and location of the coring site; COR503-37PC in the Laurentian Channel. The core location is 48°20.01'N, 61°29.99'W, at 408 m water depth. The bathymetric contour represents the 200 m isobath.

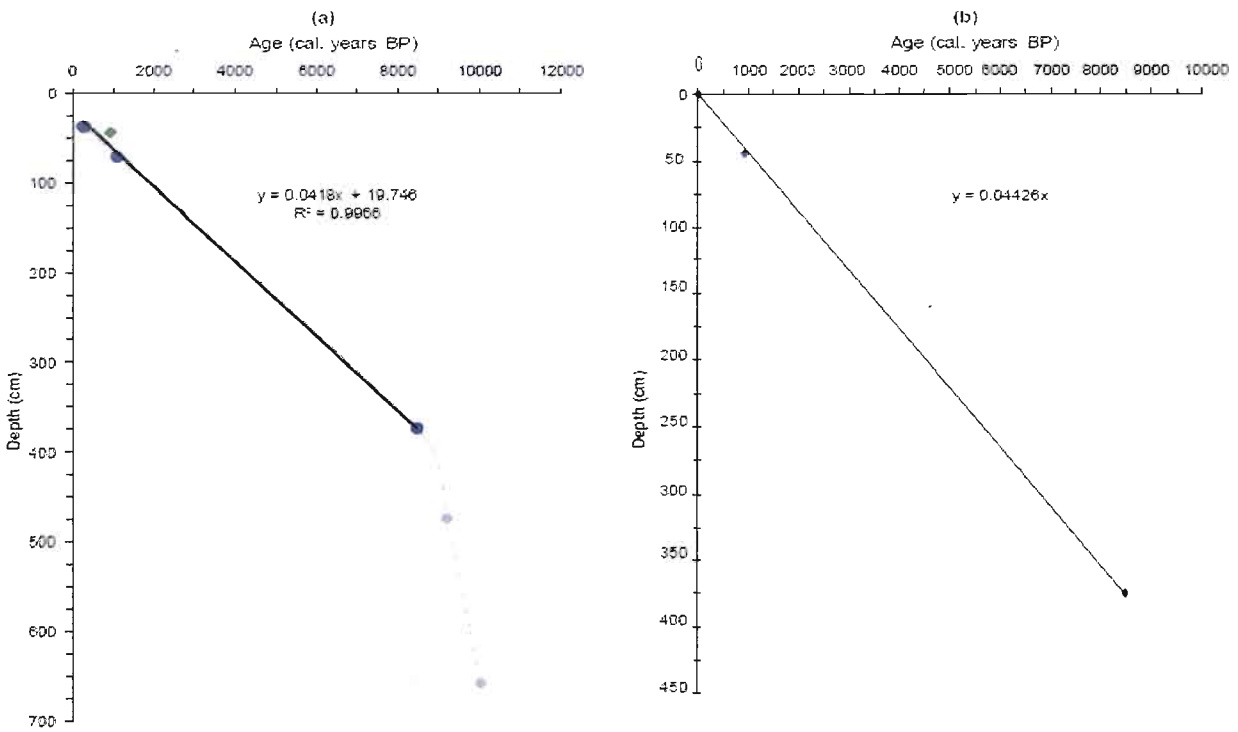

Figure 2: Chronology of COR503-37PC **a)** Age vs. depth relationship. The five circles represent calibrated ^{14}C dates from Barletta *et al.* (2010). The diamond corresponds to ^{14}C date from this study (see Table 1). The dotted grey line represents the interpolation function used by Barletta *et al.* (2010) to the set the chronology of the core. The dark line represents the linear regression used to calculate sedimentation rates across ^{14}C dates in the upper 400 cm. **b)** Age vs. depth relationship of the study section of the core. The dark line represents the linear regression used to calculate sedimentation rate across ^{14}C dates at 45 and 375 cm, assuming a 0 cal. years BP age at the top of the core.

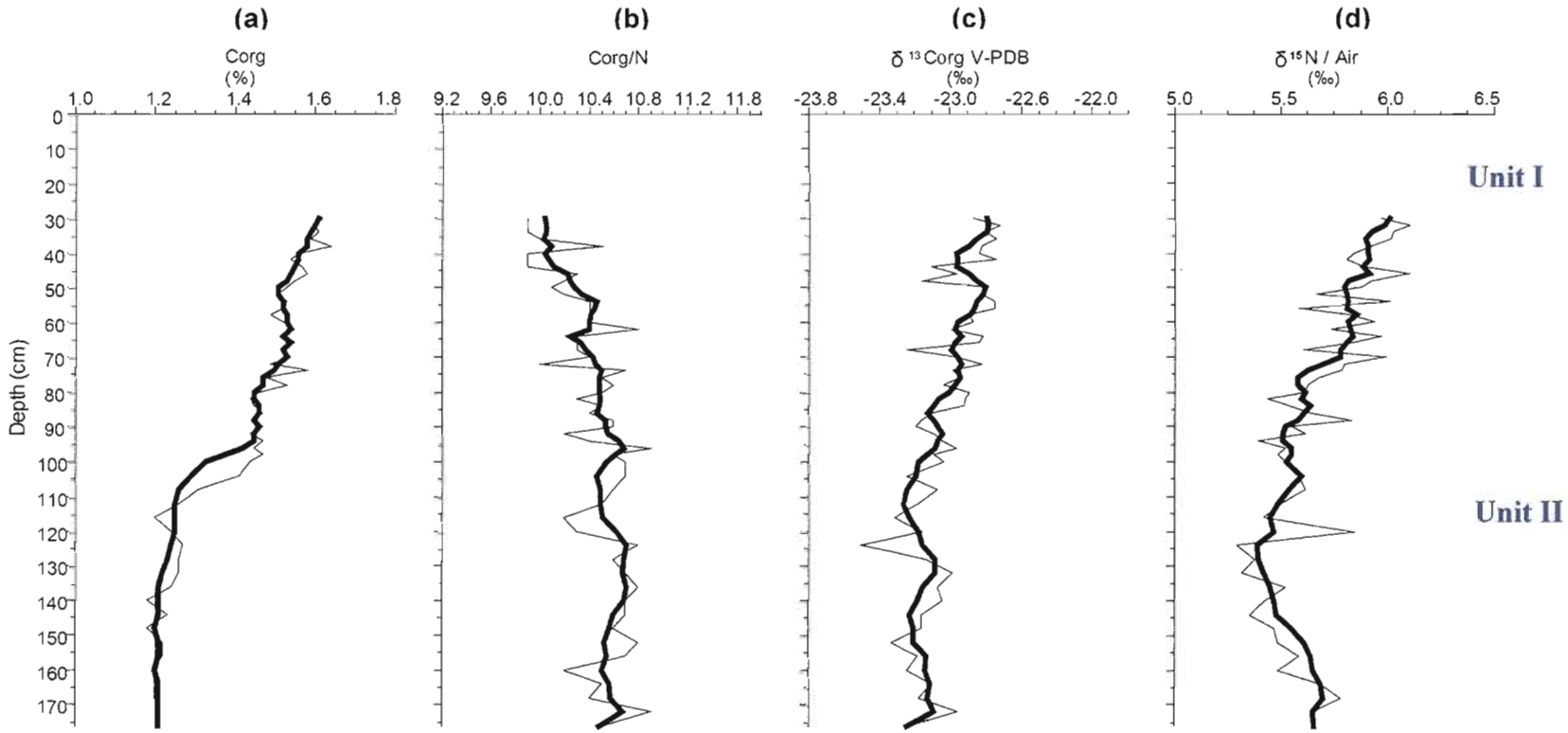

Figure 3: Geochemical and stable isotope results as function of depth (cm) in core COR503-37PC: C_{org} (organic carbon content), C_{org}/N ratio, $\delta^{13}C_{org}$ and $\delta^{15}N$. The bold curves correspond to 5-points running means. The shaded interval from 90 to 100 cm corresponds to the transition between Unit I and Unit II.

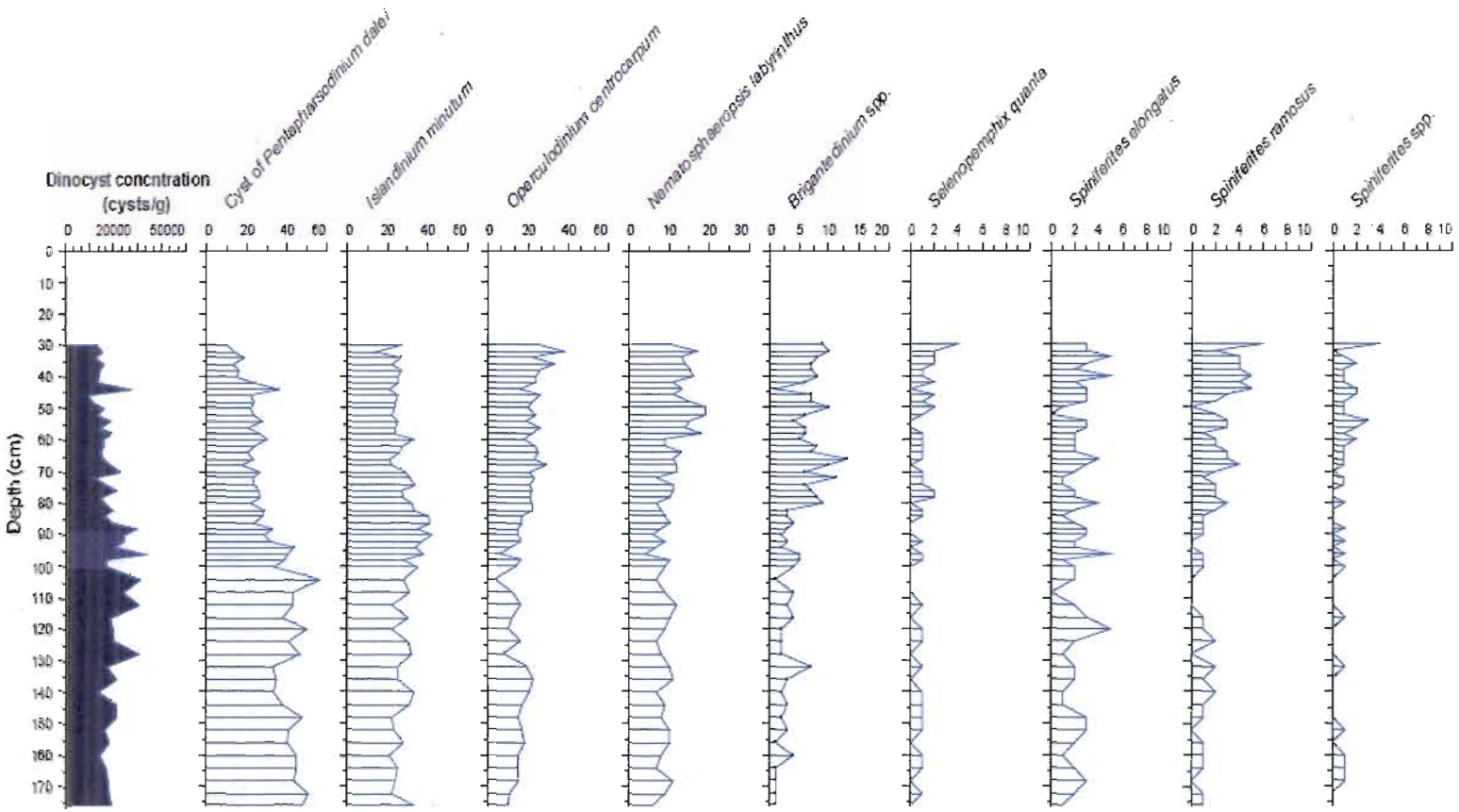

Figure 4: Dinocyst concentration (cysts g^{-1}) and the relative abundance of the main taxa as function of depth (cm) in core COR503-37PC. For information, the transition zone defined from the geochemical data (cf. Figure 3) is reported here

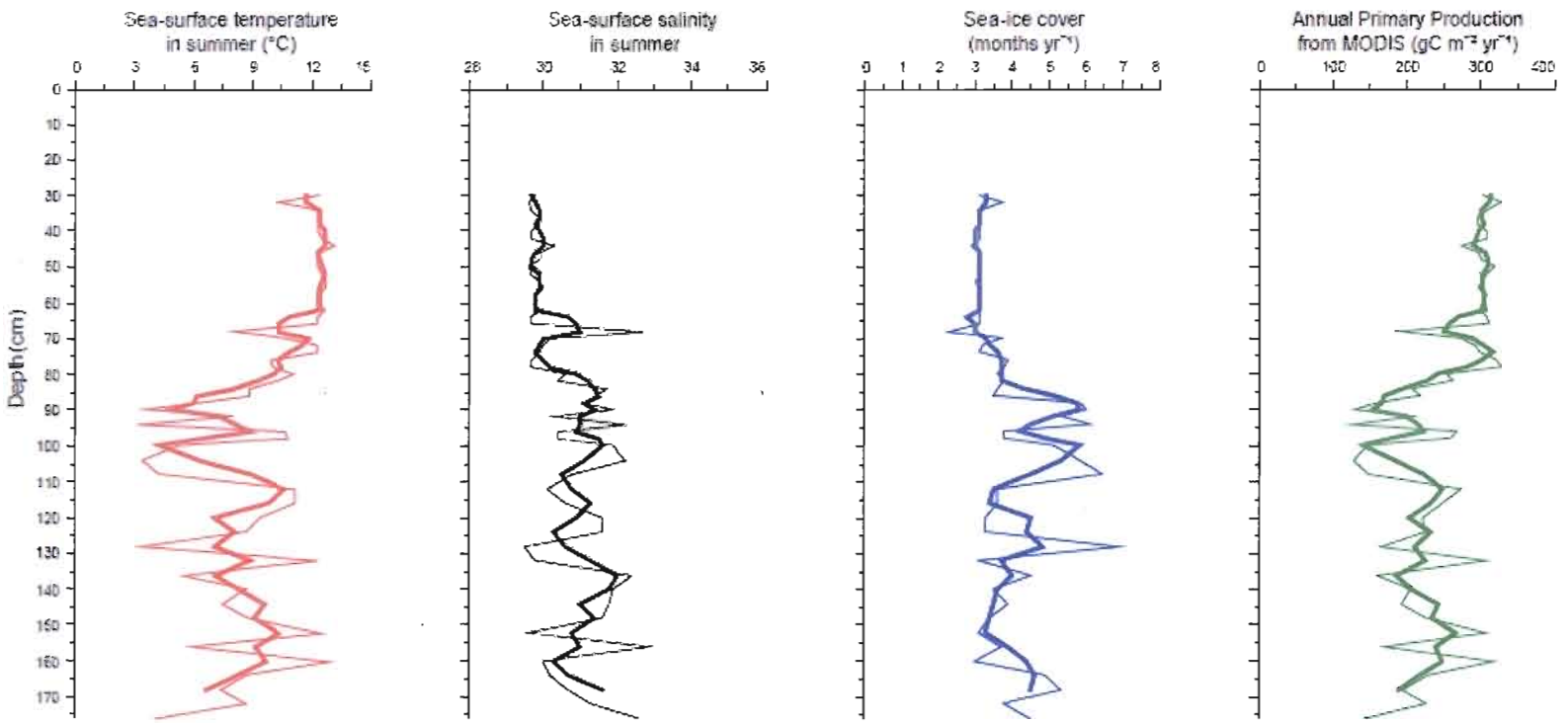

Figure 5: Reconstruction of sea-surface conditions (temperature, salinity and sea-ice cover) and annual primary production for the last 4000 years using dinocyst data from the core COR503-37PC. The reconstruction was based on the best analogue method (cf. Guiot and de Vernal, 2007) using the n= 1429 dinocyst reference data base and the reference productivity database MODIS (Behrenfeld and Falkowski, 1997). The bold curves correspond to 3-points running means. The transition zone defined from the geochemical data (cf. Figure 3) is reported here.

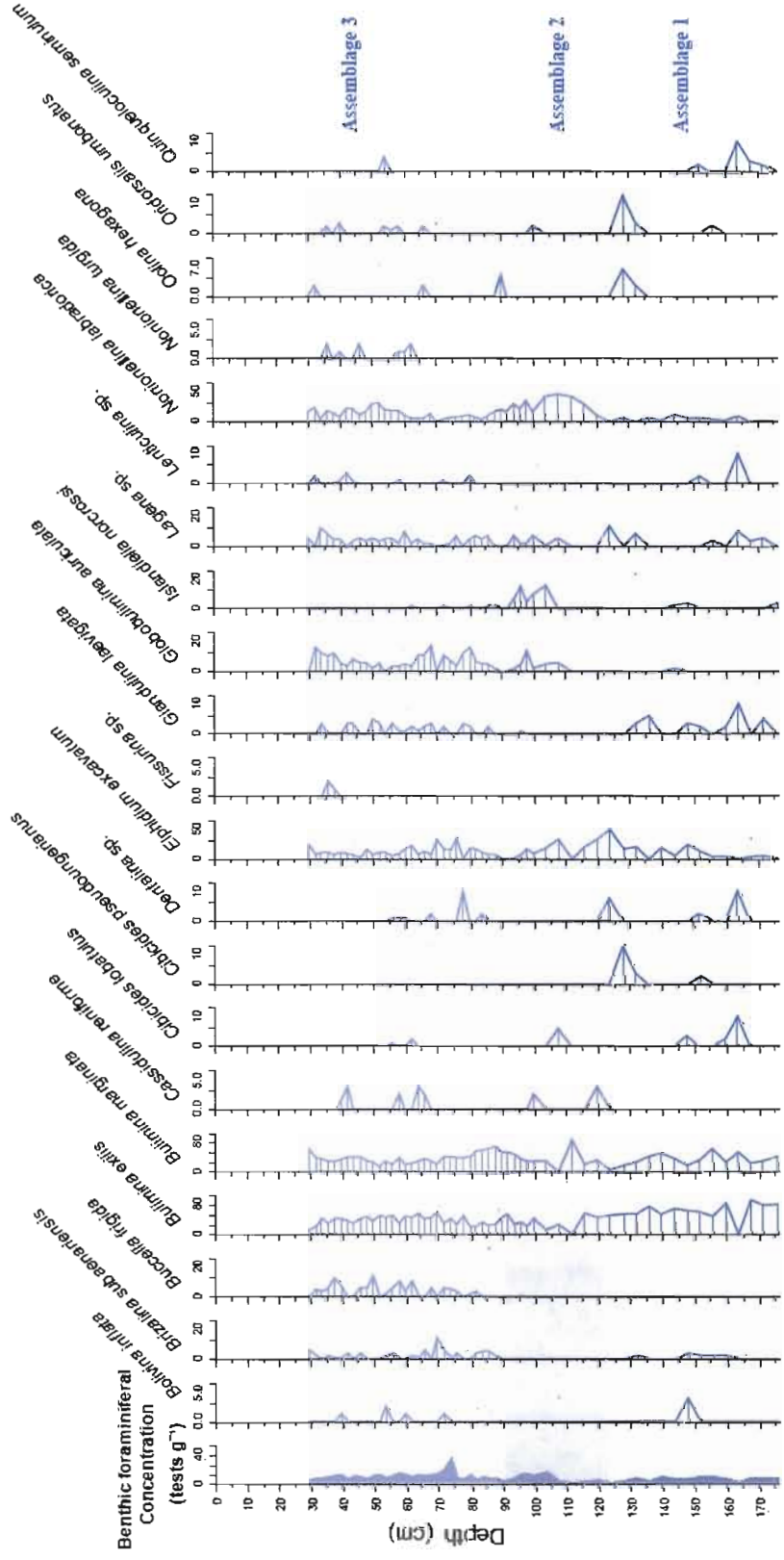

Figure 6: Summary diagram of benthic foraminifer assemblages in core COR503-37PC: concentration (tests g^{-1}) and relative abundance of taxa as function of depth (cm). The assemblages **1**, **2** and **3** are defined from the occurrence of key species *Nonionellina labradorica*, *Brizalina subaenariensis* and *Globobulimina auriculata*.

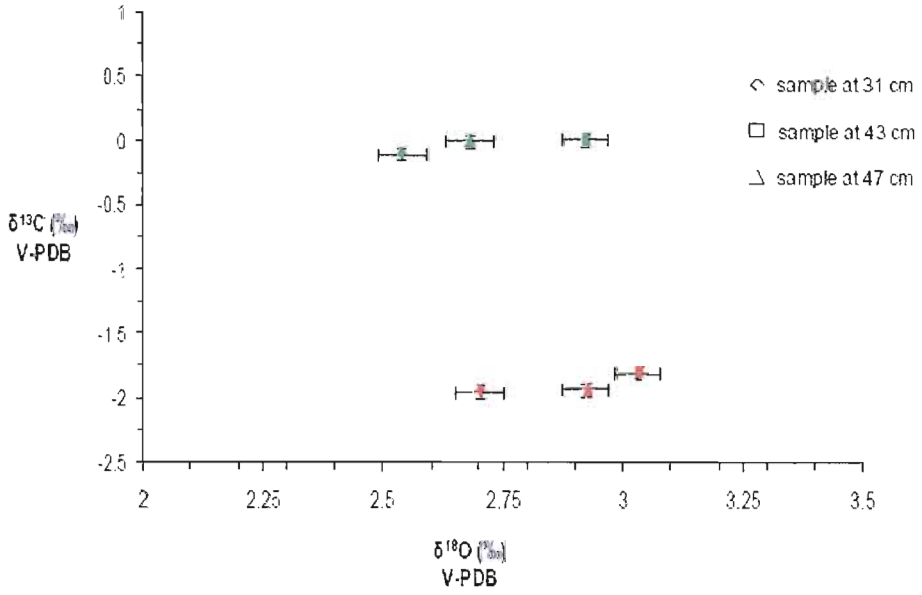

Figure 7: $\delta^{13}C$ and $\delta^{18}O$ of *Bulimina marginata* (green) and *Bulimina exilis* (red) picked in samples from COR503-37 PC (at 31, 43 and 47 cm). Analyses were performed in order to verify if we can develop a multispecies record (see Table A.3. in the supplementary data).

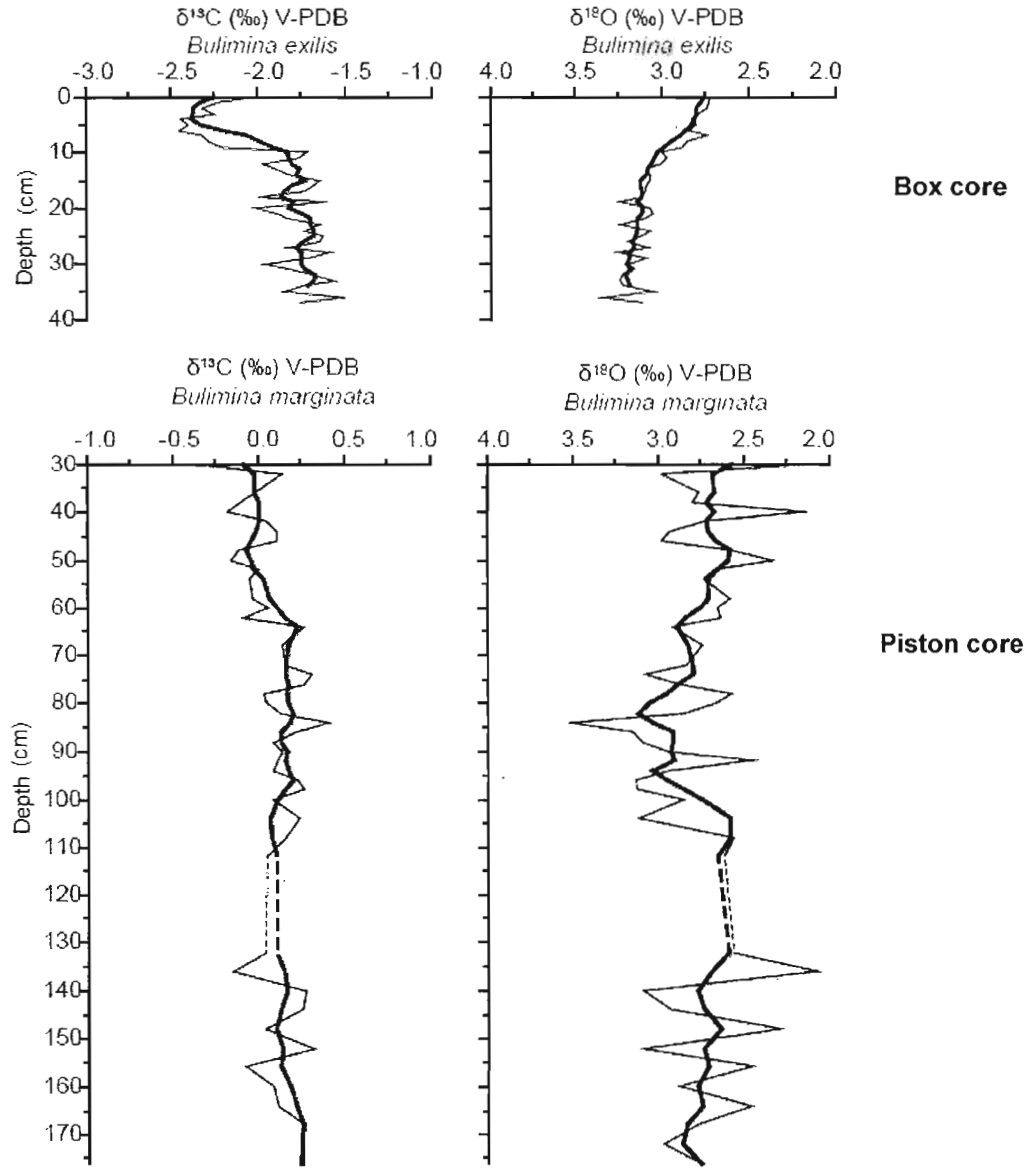

Figure 8: $\delta^{13}C$ and $\delta^{18}O$ record of benthic foraminifera *Bulimina exilis* in box core COR503-37BC (Genovesi, 2009) and *Bulimina marginata* in piston core COR503-37PC (this study) as function of depth (cm). The bold curves correspond to 5-points running mean values. Note the different $\delta^{13}C$ scale for *Bulimina exilis* and *Bulimina marginata*. The 2 ‰ difference corresponds to the discrepancy calculated from measurements in the same samples (cf. Figure 7).

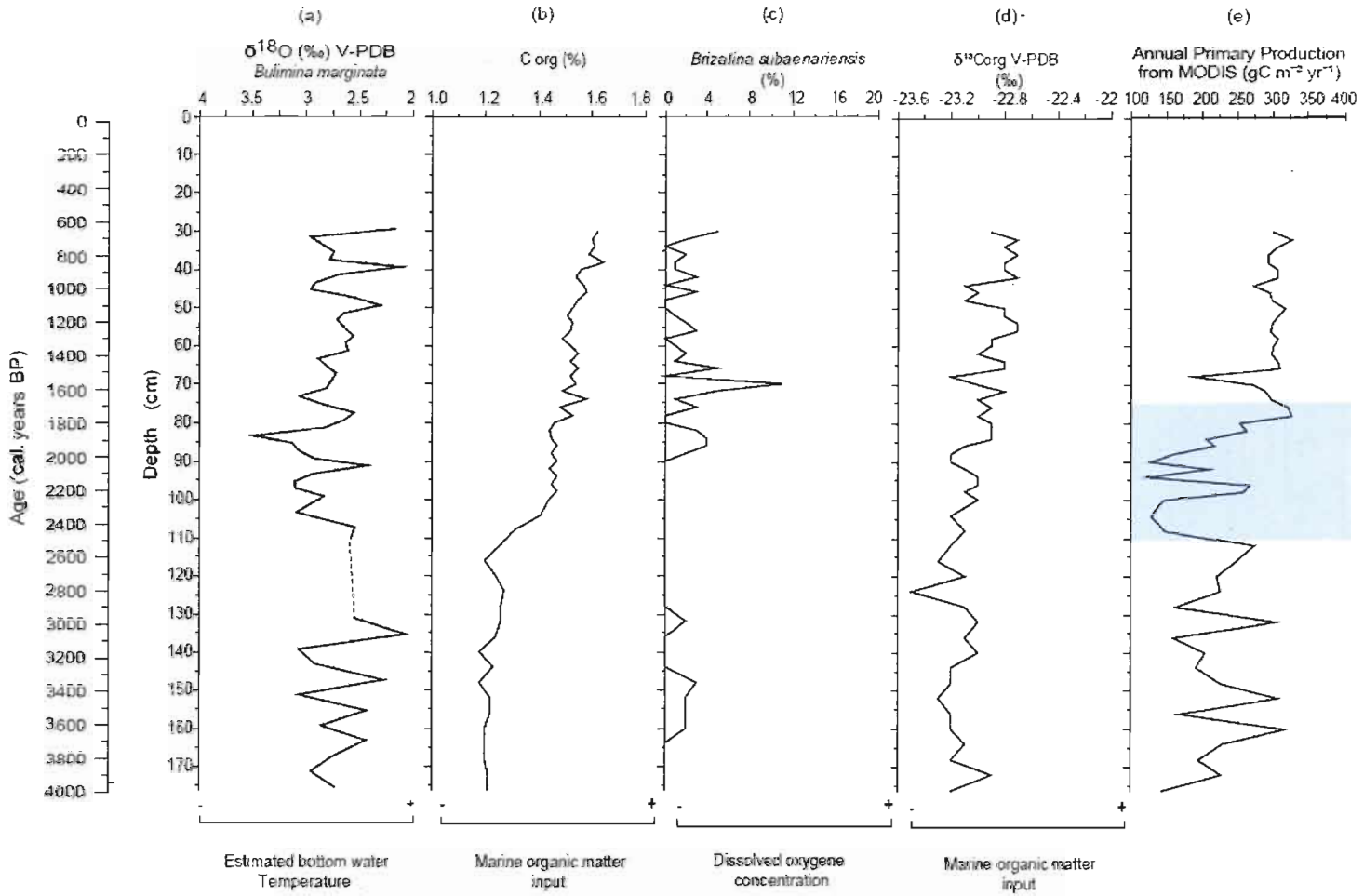

Figure 9: Summarized curves of the main proxies used to reconstruct benthic and pelagic environment in the St. Lawrence Gulf during the last 4000 years (data from COR503-37PC): a) $\delta^{18}O$ record of *Bulimina marginata;* b) Corg: Organic carbon content in the sediment; c) relative abundance of *Brizalina subaenariensis* d) $\delta^{13}C_{org}$ in the sediment; e) reconstruction of annual primary production from MODIS. The shaded interval, between 90 and 100 cm, corresponds to the transition zone defined from the geochemical data. The interval highlighted in blue (85-105 cm) corresponds to the cold period that occurred between ~1800 and 2500 cal. years BP.

Conclusion générale

Les analyses micropaléontologiques, géochimiques et isotopiques du contenu sédimentaire de la carotte COR0503-CL05-37PC échantillonnée dans le chenal Laurentien au centre du Golfe du Saint-Laurent montrent des changements importants des conditions environnementales au cours des derniers millénaires. Ces changements indiquent des variations de la productivité biogénique et des flux de matière organique, ainsi que de la température des eaux profondes et des conditions d'oxygénation du milieu benthique. Les variations que nous retraçons en milieu pélagique ne sont pas en phase avec celles qui marquent le milieu benthique. Les résultats des analyses effectuées suggèrent un changement majeur de la productivité et des flux organiques depuis ~ 2300 ans BP, alors que les données de températures suggèrent des variations millénaires avec des conditions froides enregistrées entre ~2800 et 1800 ans BP. On observe ainsi un découplage entre les variations enregistrées dans les eaux profondes et celles de surface à l'échelle des derniers millénaires. Tel n'est pas le cas dans l'Estuaire à l'échelle des derniers siècles (Thibodeau *et al.*, 2006, 2010). Dans l'Estuaire, il y a eu une diminution récente de le teneur d'oxygène dissous dans l'eau qui corresponds à la fois à une augmentation de la productivité, du flux de carbone (Thibodeau *et al.*, 2006) et à l'élévation de la température des eaux profondes pendants le dernier siècle (Thibodeau *et al.*, 2010). Dans le Golfe une productivité très élevées caractérise l'environnement pélagique après 2000 BP ans et ne semble pas avoir variée de façon significative. Par la suite la baisse récent des teneurs en oxygène dissous dans le golfe semble plutôt être liée à un réchauffement des eaux profondes (Genovesi *et al.*, soumis). Nos résultats qui se situent à une échelle de temps dépassant celle de l'occupation humaine, montrent des changements complexes de la productivité et des conditions des eaux profondes qui sont associées à des variations naturelles. En effet, ils résultent de forçages à des échelles de temps millénaires auxquelles se superposent des variations séculaires,

telles celles observées par Thibodeau *et al.* (2006, 2010) et Genovesi (2009). En outre, nos données suggèrent que les conditions caractérisant le golfe du Saint-Laurent depuis les derniers siècles, soit un réchauffement des eaux profondes et une importante productivité pélagique, sont propices à une grande sensibilité du système vis-à-vis des conditions d'oxygénation du milieu benthique.

Bibliographie générale

Barletta, F., St-onge, G., Stoner, J.S., et Lajeunesse, P., 2010. A high-resolution Holocene paleomagnetic secular variation and relative paleointensity stack from eastern Canada, Earth Planet. Sci. Lett. (2010), doi:10.1016/j.epsl.2010.07.038

Benoit, P., Gratton, Y., et Mucci, A., 2006. Modeling of dissolved oxygen levels in the bottom waters of the Lower St. Lawrence Estuary: coupling of benthic and pelagic processes. Marine Chemistry 102, 13-32.

Berhenfeld, M.J., et Falkowski, P.G., 1997. Photosynthetic rates derived from satellite based chlorophyll concentration. Limnol. Oceanogr. 42, 1-20.

Bilodeau, G., de Vernal, A., et Hillaire-Marcel, C., 1994. Benthic foraminiferal assemblages in Labrador Sea sediments: relations with deep-water mass changes since deglaciation. Can. J. Earth. Sci. 31, 128-138.

Bratton, J.F., Colman, S.M., et Seal II, R.R., 2003. Eutrophication and carbon sources in Chesapeake Bay over the last 2700 yr: Human impact in context. Geochim. Cosmochim. Acta. 67, 3385–3402.

Bugden, G.L., 1991. Changes in temperature-salinity characteristics of the deep waters of the Gulf of St. Lawrence over the past several decades. In Therriault. J.C., The Gulf of St. Lawrence: Small Ocean or a big estuary? Can.Spec.Publ.Fish.Aquat.Sci.13, 139-174.

Chabot, D., et Dutil, J.D., 1999. Reduced growth of Atlantic cod in non-lethal hypoxic conditions. J. Fish Biology, 55, 472-491.

Cloern, J.E., 2001. Our evolving conceptual model of the coastal eutrophication problem. Mar. Ecol. Prog. Ser. 210, 223-253.

Coplen, T.B., 1995. Discontinuance of SMOW and Pdb. Nature. 375, 285.

Corliss, B.H.,1985. Microhabit of benthic foraminifera within deep-sea sediments. Nature,314,151-438.

Craig, J.K., Crowder, L.B., Gray, C.D., McDaniel, C.J., Henwood, T.A., et Hanifen, J.G., 2001. Ecological effects of hypoxia on fish, sea turtles, and marine mammals in the northwestern Gulf of Mexico. *In.* Costal Hypoxia: consequences for living

resources and ecosystems. Coastal and Estuarine Studies 58. American Geophysical Union, Washington D.C, 269-292.

de Vernal, A., Guiot, J., et Turon, J.L., 1993. Late and postglacial paleoenvironments of the Gulf of St. Lawrence: Marine and terrestrial palynological evidence. Géographie physique et Quaternaire 42 (2), 167-180.

de Vernal, A., Henry, M., et Bilodeau, G., 1996. Techniques de préparation et d'analyse en micropaléontologie. Les cahiers du GEOTOP. Unpublished report. http://gizmo.geotop.uqam.ca//Gestion_Documents/Cahiers/Micropaleontologie_cahier3.pdf

de Vernal, A., Rochon, A., Turon, J.-L., et Matthiessen, J., 1997. Organic-walled dinoflagellate cysts: palynological tracers of seasurface conditions in middle to high latitude marine environments. Geobios, 30, 905–920.

de Vernal, A., Henry, M., Matthiessen, J., Mudie, P.J., Rochon, A., Boessenkool, K.P., Eynaud, F., Grosfjeld, K., Guiot, J. et Hamel, D., 2001. Dinoflagellate cyst assemblages as tracers of sea-surface conditions in the northern North Atlantic, Arctic and sub-Arctic seas: the new" n= 677" data base and its application for quantitative paleoceanographic reconstruction. Journal of Quaternary Science, 16(7), 681-698.

de Vernal, A., Eynauld, F., Henry, M., Hillaire-Marcel, C., Londeix, L., Mangin, S., Matthiessen, J., Marret, F., Radi, T., Rochon, A., Solignac, S., et Turon, J.L., 2005. Reconstruction of sea-surface conditions at middle to high latitudes of the Northern Hemisphere during the Last Glacial Maximum (LGM) based on dinoflagellate cyst assemblages. Quaternary Science Reviews. 24, 897–924.

de Vernal, A., et Marret, F., 2007. Organic-Walled Dinoflagellate Cysts:Tracers of Sea-Surface Conditions. *In,* Hillaire-Marcel, C., and de Vernal, A., (Ed). 2007. Developments in marine geology Volume1: Proxies in late Cenozoic paleoceanography, GEOTOP. Université du Québec à Montréal, Québec, Chapter9, 371-408.

den Dulk, M.., Reichart, G.J., van Heyst, S., Zachariasse, W.J., et Vaen der Zwaan, G.J., 2000. Benthic foraminifera as proxies of organic matter flux and bottom water oxygenation? A case history from the northern Arabian Sea. Palaeogeography, Palaeoclimatology, Palaeoecology, 161,337–359.

Diaz, R., et Rosenberg, R., 1995. Marine benthic hypoxia: a review of its ecological effects and the behaviour responses of benthic macrofauna.Oceanogr. Mar. Biol. Annu, Rev, 33, 245-303

Diaz, R., et Rosenberg, R., 2008. Spreading dead zones and consequences for marine ecosystems. Science, 321, 926-929.

Dickie, L., et Trites, L.M. 1983. The Gulf of St. Lawrence. *In* Estuaries and enclosed seas. (Ed) B.H. Ketchum. Elsevier, Amsterdam, The Netherlands. pp, 403–425.

El Sabh, M., 1973. Seasonal and long term variations of the water properties in the Gulf of St. Lawrence . *In* El Sabh, M., [ed]. Proc. Workshop Physical sciences in the Gulf of St. Lawrence. pp, 128-158.

Fontanier, C., Jorissen, F.J., Licari, L., Alexandre, A., Anschutz, P., et Carbonel, P., 2002. Live benthic foraminiferal faunas from the Bay of Biscay: faunal density, composition, and microhabitats. Deep-Sea Research I 49, 751–785.

François, R., Altabet, M.A., Yu, E.F., Sigman, D.M., Bacon, M.P., Frank, M., Bohrmann, G., Bareille, G., et Labeyrie, L.D., 1997. Contribution of Southern Ocean surface-water stratification to low atmospheric CO_2 concentrations during the last glacial period. Nature, 389, 929-935.

Genovesi, L., 2009. Indices micropaléontologiques et géochimiques de changements récents de l'oxygénation et la température des eaux profondes du Golfe du ST-Laurent. Msc. Thesis. Université du Québec à Montréal, 71pp.

Genovesi, L., de Vernal, A., Thibodeau, B., Hillaire-Marcel, C., Mucci, A., et Gilbert, D., *soumis*. Recent changes in bottom water oxygenation and temperature in the Gulf of St. Lawrence: micropaleontological and geochemical evidence.

Gilbert, D., et Pettigrew, B., 1997. Inetrannual variability the CIL core temperature in the Gulf of St. Lawrence. Can. J. Fish. Aquat. Sci. 54 (1), 57-67.

Gilbert, D., Sundby, B., Gobeil, C., Mucci, A,. et Tremblay, G-H., 2005. A seventy-two-year record of diminishing deep water oxygen in the St Lawrence estuary: The Northwest Atlantic connection. Limnol. Oceanogr. 50, 1654-1666.

Gilbert, D., Chabot, D., Archambaut, P., Rondeau, B., et Herbert, S., 2007. Appauvrissement en oxygène dissous dans les eaux profondes du Saint-Laurent marin : Causes possibles et impacts écologiques. Le Naturaliste Canadien, 131 (1), 67-75.

Gilbert, D., Rabalais, N.N., Diaz, R.J., et Zhang, J., 2010. Evidence for greater oxygen decline rates in the coastal ocean than in the open ocean. Biogeosciences, 7, 2283-2296.

Guiot, J., et de Vernal, A., 2007. Transfert functions: methods for quantitative paeleoceanography based on microfossils. *In,* Hillaire-Marcel, C., and de Vernal, A., (Ed). 2007. Developments in marine geology Volume1: Proxies in late Cenozoic paleoceanography, GEOTOP. Université du Québec à Montréal, Québec, Chapter 13, 523-563.

Hélie, J.F., 2009. Elemental and stable isotopic approaches for studying the organic and inorganic carbon components in natural samples. From Deep-Sea to Coastal Zones: Methods – Techniques for Studying Paleoenvironments, IOP Conference Series: Earth and Environmental Science, 5, 012005, doi:10.1088/1755-1307/5/1/012005

Hughen, K. A., Baillie, M.G.L., Bard, E., Bayliss, A., Beck, J.W., Blackwell, P.G., Buck, C.E., Burr, G.S., Cutler, K.B., Damon, P.E., Edwards, R.L., Fairbanks, R.G., Friedrich, M., Guilderson, T.P., Herring, C., Kromer, B., McCormac, F.G., Manning, S.W., Ramsey, C.B., Reimer, P.J., Reimer, R.W., Remmele, S., Southon, J.R., Stuiver, M., Talamo, S., Taylor, F.W., van der Plicht, J., et Weyhenmeyer, C.E. 2004. Marine04 Marine radiocarbon age calibration, 26 - 0 ka BP. Radiocarbon 46, 1059-1086.

Jorissen, F.J., Wittling, I., Peypouquet, J.P., Rabouille, C., et Relexans, J.C., 1998. Live benthic foraminiferal faunas off Cape Blanc, NW Africa; Community structure and microhabitats. Deep-Sea Res., I 45, 2157-2188.

Jorissen, F.J, 1999. Benthic foraminiferal successions across Late Quaternary Mediterranean sapropels. Marine Geology 153, 91–101.

Jorissen, F.J, Fontanier, C., et Thomas, E., 2007. Paleoceanographical proxies based on deep-sea Benthic foraminiferal assemblage characteristics. *In,* Hillaire-Marcel, C., and de Vernal, A., (Ed). 2007. Developments in marine geology Volume1: Proxies in late Cenozoic paleoceanography, GEOTOP. Université du Québec à Montréal, Québec, Chapter 7, 263-325.

Kaiho, K., 1994. Benthic foraminiferal dissolved-oxygen index and dissolved-oxygen levels in the modern ocean. Geology 22, 719-722.

Keeling, R.F., et Garcia, H.E., 2002. The change in Oceanic O_2 inventory associated with recent global warming, P.Natl.Acad.Sci. USA, 99 (12),7848-7853: doi: 10.1073/pnas.122154899.

Leckie, R.M., et Olson, H.C., 2003. Foraminifera as proxies for sea-level Change on siliciclastic margins. Micropaleontologic proxies for seal-level Change and stratigraphic Discontinuities. SPEM. 75, 5-19.

Loring, D.H., et Nota, D.J.G., 1973. Morphology and sediments of the Gulf of St.Lawrence. Bull. Fish. Res. Bd Can.182, pp147.

Matthews, J., 1969. The assessment of a method for the determination of absolute pollen frequencies. New Phytologist68 (1), 161-166.

McKay, J.L., Pedersen, T.F., et Kienast, S.S., 2004. Organic carbon accumulation over the last 16 kyr off Vancouver Island, Canada: evidence for increased marine productivity during the deglacial. Quaternary Science Reviews, 23, 261–281.

Meyers, P.A., 1994. Preservation of elemental and isotopic source identification of sedimentary organic matter. Chem.Geol, 114, 289-302.

Meyers, P.A, 1997. Organic geochemical proxies of paleoceanographic, paleolimnologic, and paleoclimatic processes. Org. Geochem. 27, N^0 5/6, 213-250.

Mojtahid. M., Jorissen, F., et Person, T.H., 2008. Comparison of benthic foraminiferal and macrofaunal responses to organic pollution in the Firth of Clyde (Scotland). Marine Pollution Bulletin, 56, 42–76.

Montoya, J.P., 1994. Nitrogen isotope fractionation in the modern ocean: implications for the sedimentary record. *In*: Zahn, R., Pedersen, T.F., Kaminski, M.A., Labeyrie, L. (Eds.), Carbon Cycling in the Glacial Ocean: Constraints on the Ocean's Role in Global Change. NATO ASI Series, Vol. 117. Springer, Berlin, pp 259–279.

Mucci, A., Sundby, B., Gehlen, M., Arakaki, T., Zhong, S., et Silverberg, N., 2000.The fate of carbon in continental shelf sediments of eastern Canada: a case study. Deep-sea Research II (47), 733-760.

Murray, J.W., et Alve, E., 1999. Taphonomic experiments on marginal marine foraminiferal assemblages: how much ecological information is preserved? Palaeogeography, Palaeoclimatology, Palaeoecology ,149, 183–197.

Murray, J.W., 2001. The niche of benthic foraminifera, critical thresholds and proxies. Marine Micropaleontology, 41, 1-7.

Muzuka, A.N.N., et Hillaire-Marcel, C. 1999. Burial rates of organic matter along the eastern Canadian margin and stable isotope constraints on its origin and diagenetic evolution. Mar. Geol., 160, 251-27.

Osterman, L.E., 2003. Benthic foraminifers from the continental shelf and slope of the Gulf of Mexico: an indicator of shelf hypoxia. Estuarine, Coastal and Shelf Science, 58, 17–35.

Osterman, L.E., Poore, R.Z., Swarzenski, P.W., Senn, D.B., et DiMarco, S.F., 2009. The 20th-century development and expansion of Louisiana shelf hypoxia, Gulf of Mexico. Geo-Mar. Lett., 29, 405–414.

Radi, T., Pospelova, V., de Vernal, A., et Barrie, J.V., 2007. Dinoflagellate cysts as indicators of water quality and productivity in British Columbia estuarine environments. Marine Micropaleontology, 62, 269-297.

Radi, T., et de Vernal, A., 2008. Dinocysts as proxy of primary productivity in mid-high latitudes of the Northen Hemisphere. Marine Micropaleontology, 68, 84-114.

Ravelo, A., et Hillaire-Marcel, C., 2007. The use of Oxygen and Carbon isotopes of foraminifera in paleoceanography. *In,* Hillaire-Marcel, C., and de Vernal, A., (Ed). 2007. Developments in marine geology Volume1: Proxies in late Cenozoic paleoceanography, GEOTOP. Université du Québec à Montréal, Québec, Chapter18,735-764.

Rochon, A., de Vernal, A., Turon, J.L., Matthiessen, J., et Head, M.J., 1999. Distribution of recent dinoflagellate cysts in surface sediments from the North Atlantic ocean and adjacent seas inrelation to sea-surface parameters. Am. Assoc. Stratigr. Palynol. Found. 35.152p.

Rodrigues, C.G., 1980. Holocene microfauna and paleoceanography of the Gulf of St. Lawrence. Ph.D. Thesis. Carleton University.

Saucier, F.J., Roy, F., Gilbert, D., Pellerin, P., et Ritchie, H., 2003. The formation and circulation process of water masses in the Gulf of St.Lawrence. J.Geo.Res.108, 3269-3289.

Savenkoff, C., Vézina, A.F., Packard, T.T., Silverbeg, N., Therriault, J.C., Chen, W., Bérubé, C., Mucci, A., Klein, B., Mesplé, F., Tremblay, J.E., Legendre, L., Wesson, J., et Ingram, R.G., 1996. Distributions of oxygen, carbon, and respiratory activity in the deep layer of the Gulf of St. Lawrence and their implications for the carbon cycle. Can. J. Fish. Aquat. Sci., 53, 2451–2465.

Schmidt, G.A., Bigg, G. R., et Rohling, E. J. 1999. Global Seawater Oxygen-18 Database. http://data.giss.nasa.gov/o18data/

Sen Gupta, B.K., et Machain-Castillo, M.L., 1993. Benthic foraminifera in oxygen-poor-habitats.Marine Micropaleontology, 20, 183-201.

Shackleton, N.J., 1974. Attainment of isotopic equilibrium between ocean water and the benthonic foraminifera genus Uvigerina: isotopic changes in the ocean during the last glacial. *In* J. Labeyrie [ed], Méthodes quantitatives d'études des variations du climat au cours du Pléistocène, Éditions du CNRS. p.203-209.

Stuiver, M., Reimer, P.J., et Reimer, R.W., 2005. CALIB 5.0. Available from http://calib.qub.ac.uk/calib/

Thibodeau, B., de Vernal, A., and Mucci, A., 2006. Recent eutrophication and consequent hypoxia in the bottom waters of the Lower St. Lawrence Estuary: Micropaleontological and geochemical evidence. Marine Geology, 231, 37-50.

Thibodeau, B., de Vernal, A., Hillaire-Marcel, C., and Mucci, A., ***In Press***. 20th Century warming in deep waters of the Gulf of St. Lawrence: a unique feature of the last millennium, *Geophysical Research Letters*.

Verity, P.G., Alber, M., et Bricker, S.B., 2006. Development of hypoxia in well-mixed subtropical estuaries in the southeastern USA. Estuary. Coasts 29, 665–673.

Waelbroeck, C., Labeyrie, L., Michel, E., Duplessy, J.C., Mc Manus, J.F., Lambeck, K., Balbon, E., et Labracherie, M., 2002. Sea-level and deep water temperature changes derived from benthic foraminifera isotopic records. Quaternary Science Reviews, 21, 295-305.

Wu, R.S.S., 2002. Hypoxia: from molecular responses to ecosystem responses. Marine Pollution Bulletin, 45, 35-45.

ANNEXE A

Résultats des analyses géochimiques et isotopiques dans la carotte COR0503-CL05-37PC

Tableau A.1
Résultats d'analyses géochimiques et isotopiques effectuées sur la matière organique dans la carotte COR0503-CL05-37PC

Profondeur (cm)	C_{org} (%)	C/N	$\delta^{13}C_{org}$ V-PDB (‰)	$\delta^{15}N$ / AIR (‰)
30	1,62	9,9	-22,87	5,97
32	1,60	9,9	-22,72	6,11
34	1,61	9,9	-22,80	6,03
36	1,59	10,0	-22,74	6,02
38	1,64	10,5	-22,82	5,93
40	1,56	9,9	-22,83	5,85
42	1,54	9,9	-22,74	5,81
44	1,57	9,9	-23,10	5,89
46	1,58	10,3	-22,96	6,10
48	1,55	10,2	-23,15	5,93
50	1,53	10,1	-22,79	5,88
52	1,51	10,2	-22,82	5,67
54	1,53	10,4	-22,75	6,02
56	1,52	10,4	-22,75	5,60
58	1,49	10,4	-22,89	5,82
60	1,52	10,4	-22,87	5,94
62	1,55	10,8	-22,99	5,74
64	1,52	10,3	-22,81	5,97
66	1,55	10,3	-22,83	5,85
68	1,52	10,3	-23,23	5,62
70	1,54	10,4	-22,97	5,99
72	1,49	10,0	-22,82	5,80
74	1,58	10,7	-22,98	5,79
76	1,48	10,5	-22,94	5,68
78	1,53	10,6	-23,03	5,63
80	1,46	10,5	-22,89	5,62
82	1,44	10,3	-22,91	5,44
84	1,45	10,5	-22,92	5,54
86	1,47	10,4	-23,10	5,64
88	1,45	10,6	-23,16	5,83
90	1,47	10,6	-23,19	5,55
92	1,44	10,2	-23,09	5,62
94	1,47	10,4	-23,04	5,40
96	1,45	10,9	-22,96	5,52
98	1,47	10,6	-23,09	5,49
100	1,44	10,7	-23,03	5,52
104	1,41	10,7	-23,24	5,59
108	1,31	10,6	-23,07	5,62

Tableau A.1 (suite)
Résultats d'analyses géochimiques et isotopiques effectuées sur la matière organique dans la carotte COR0503-CL05-37PC

Profondeur (cm)	C_{org} (%)	C/N	$\delta^{13}C_{org}$ V-PDB (‰)	$\delta^{15}N$ / AIR (‰)
112	1,26	10,5	-23,18	5,50
116	1,20	10,2	-23,31	5,42
120	1,24	10,3	-23,15	5,85
124	1,27	10,8	-23,50	5,30
128	1,26	10,6	-23,13	5,38
132	1,26	10,7	-22,98	5,32
136	1,24	10,8	-23,07	5,52
140	1,18	10,7	-23,04	5,43
144	1,23	10,7	-23,16	5,36
148	1,18	10,6	-23,16	5,47
152	1,22	10,8	-23,33	5,49
156	1,22	10,7	-23,18	5,59
160	1,20	10,2	-23,24	5,49
164	1,20	10,5	-23,10	5,69
168	1,20	10,4	-23,17	5,78
172	1,21	10,9	-22,95	5,65
176	1,21	10,5	-23,24	5,66

Tableau A.2.
Résultats d'analyses isotopiques ($\delta^{13}C$ et $\delta^{18}O$) dans les tests carbonatés du foraminifère benthique *Bulimina marginata* de la carotte COR0503-CL05-37PC

Profondeur (cm)	$\delta^{13}C$ V-PDB (‰)	$\delta^{18}O$ V-PDB (‰)
30	-0,32	2,19
32	0,14	2,98
34	-	-
36	-0,01	2,76
38	-0,10	2,80
40	-0,18	2,13
42	0,05	2,72
44	0,11	2,93
46	0,11	2,98
48	-0,11	2,58
50	-0,16	2,32
52	0,00	2,67
54	-0,05	2,73
56	-	-
58	-0,03	2,58
60	0,06	2,65
62	-0,09	2,63
64	0,27	2,91
66	-	-
68	0,14	2,74
70	-	-
72	0,16	2,83
74	0,31	3,08
76	0,27	2,86
78	0,03	2,57
80	0,05	2,66
82	0,13	2,85
84	0,41	3,52
86	0,22	3,15
88	0,09	3,09
90	0,14	2,94
92	0,11	2,45
94	0,09	2,94
96	0,23	3,13
98	0,27	3,12
100	0,09	2,85
104	0,24	3,11

Tableau A.2. (suite)
Résultats d'analyses isotopiques ($\delta^{13}C$ et $\delta^{18}O$) dans les tests carbonatés du foraminifère benthique *Bulimina marginata* de la carotte COR0503-CL05-37PC

Profondeur (cm)	$\delta^{13}C$ V-PDB (‰)	$\delta^{18}O$ V-PDB (‰)
108	0,16	2,56
112	0,05	2,61
116	-	-
120	-	-
124	-	-
128	-	v
132	0,04	2,56
136	-0,15	2,08
140	0,28	3,09
144	0,26	2,93
148	0,04	2,29
152	0,32	3,09
156	-0,08	2,45
160	0,09	2,88
164	0,11	2,46
168	0,27	2,77
172	0,25	2,97
176	0,25	2,75

Tableau A.3.
Résultats d'analyses isotopiques ($\delta^{13}C$ et $\delta^{18}O$) dans les tests carbonatés de foraminifères benthiques *Bulimina marginata* et *Bulimina marginata* de la carotte COR0503-CL05-37PC

	Bulimina exilis		*Bulimina marginata*	
Profondeur (cm)	**$\delta^{13}C$ V-PDB (‰)**	**$\delta^{18}O$ V-PDB (‰)**	**$\delta^{13}C$ V-PDB (‰)**	**$\delta^{18}O$ V-PDB (‰)**
31	-1,95	2,70	-0,10	2,54
39	-1,80	2,91	-	-
43	-1,81	3,03	0,01	2,92
47	-1,93	2,92	0,00	2,68
49	-1,94	3,08	-	-

ANNEXE B

Dénombrement et concentrations des palynomorphes marins et terrestres dans la carotte COR0503-CL05-37PC

Tableau B.1.
Dénombrement des dinokystes dans la carotte COR0503-CL05-37PC

Profondeur (cm)	30	32	34	36	38	40	42	44	46	48	50	52	54	56
Operculodinium centrocarpum	76	113	65	99	77	73	62	49	68	57	55	67	54	68
Ocentrocarpum centrocarpum court processus	6	2	0	0	0	0	2	7	0	3	2	0	1	0
Nematosphaeropsis labyrinthus	32	52	38	41	45	48	29	38	29	38	51	51	41	36
Islandinium minutum	84	42	80	67	82	74	66	64	67	63	62	61	69	63
Islandinium? cezare	0	0	0	0	0	0	0	0	0	0	0	0	0	0
Kyste de *Pentapharsodinium dalei*	32	42	57	39	49	45	63	108	57	61	58	67	79	55
Brigantedinium spp.	29	31	24	20	21	23	16	4	18	19	28	17	11	17
Selenopemphix quanta	12	5	7	5	3	4	4	0	4	2	6	3	1	1
Spiniferites elongatus	10	8	15	10	7	16	6	9	8	7	4	1	7	9
Spiniferites ramosus	17	5	11	13	12	14	10	15	8	5	1	6	8	8
Spiniferites mirabilis-hyperacanthus	0	0	0	0	0	0	0	0	0	0	0	0	0	0
Spiniferites spp.	11	0	4	6	4	4	2	7	4	3	2	2	7	6
Ataxiodinium choane	0	0	0	0	0	0	0	0	0	0	0	0	0	0
c.f Alexandrium tamarense type Kyste	0	0	0	0	0	0	2	0	0	0	2	4	0	0
Total	309	300	301	300	300	301	260	301	263	258	269	275	278	263

Tableau B.1. (suite)
Dénombrement des dinokystes dans la carotte COR0503-CL05-37PC

Profondeur (cm)	58	60	62	64	66	68	70	72	74	76	78	80	82	84
Operculodinium centrocarpum	65	54	73	77	70	88	64	70	63	71	68	69	65	51
Ocentrocarpum centrocarpum court processus	0	0	0	0	0	0	0	0	0	0	0	0	0	0
Nematosphaeropsis labyrinthus	54	26	27	41	32	37	36	21	35	36	31	21	25	28
Islandinium minutum	69	99	83	80	62	65	87	93	104	88	91	102	99	124
Islandinium? cezare	0	0	0	0	0	0	0	0	0	0	0	0	0	0
Kyste de *Pentapharsodinium dalei*	82	89	74	66	70	55	81	70	72	85	86	70	89	87
Brigantedinium spp.	17	14	25	21	38	29	18	32	17	21	26	28	8	10
Selenopemphix quanta	2	3	4	4	3	0	3	3	4	6	6	1	3	2
Spiniferites elongatus	5	5	5	7	12	9	6	4	2	8	6	13	6	3
Spiniferites ramosus	3	5	6	8	10	11	5	4	5	6	5	8	6	2
Spiniferites mirabilis-hyperacanthus	0	0	1	1	1	4	0	1	0	0	1	0	0	0
Spiniferites spp.	3	6	4	3	3	2	1	3	4	0	0	3	1	0
Ataxiodinium choane	0	0	1	0	0	0	0	0	0	0	0	0	0	0
c.f Alexandrium tamarense type Kyste	0	0	0	0	0	0	0	0	0	0	0	0	0	0
Total	300	301	303	308	301	300	301	301	306	321	320	315	302	307

Tableau B.1. (suite)
Dénombrement des dinokystes dans la carotte COR0503-CL05-37PC

Profondeur (cm)	86	88	90	92	94	96	98	100	104	108	112	116	120	124
Operculodinium centrocarpum	52	45	47	48	35	18	48	42	13	35	51	37	33	49
Ocentrocarpum centrocarpum court processus	0	7	5	1	2	1	1	2	0	1	4	4	0	1
Nematosphaeropsis labyrinthus	32	25	17	27	20	11	29	27	21	28	37	31	27	23
Islandinium minutum	125	107	128	113	101	114	84	108	85	93	70	97	69	93
Islandinium? cezare	0	0	0	0	0	0	0	0	0	0	1	0	0	0
Kyste de *Pentapharsodinium dalei*	73	101	90	99	132	123	117	103	174	132	135	122	157	130
Brigantedinium spp.	12	9	7	9	5	15	14	12	4	12	8	13	7	5
Selenopemphix quanta	1	0	0	2	0	2	2	0	0	1	4	1	2	3
Spiniferites elongatus	6	8	8	6	5	14	4	6	6	1	5	8	17	6
Spiniferites ramosus	4	3	3	1	0	4	2	4	1	0	1	3	2	5
Spiniferites mirabilis-hyperacanthus	2	0	0	0	0	0	0	1	0	0	0	0	0	0
Spiniferites spp.	1	3	1	3	0	2	1	2	0	1	1	2	0	0
Ataxiodinium choane	0	0	0	0	0	0	0	0	0	0	0	1	1	0
c.f Alexandrium tamarense type Kyste	0	0	0	0	0	0	0	0	0	0	0	0		0
Total	308	308	306	309	300	304	302	307	304	304	317	319	315	315

Tableau B.1. (suite)
Dénombrement des dinokystes dans la carotte COR0503-CL05-37PC

Profondeur (cm)	128	132	136	140	144	148	152	156	160	164	168	172	176
Operculodinium centrocarpum	24	58	68	60	54	46	47	54	42	45	42	32	26
Ocentrocarpum centrocarpum court processus	0	0	3	0	0	0	3	0	1	5	0	1	2
Nematosphaeropsis labyrinthus	23	29	33	21	30	24	26	31	23	21	31	25	15
Islandinium minutum	95	76	76	100	100	68	62	82	58	72	100	82	90
Islandinium? cezare	4	0	0	0	0	0	0	0	1	0	3	3	0
Kyste de *Pentapharsodinium dalei*	142	101	108	103	121	147	113	120	122	133	166	163	130
Brigantedinium spp.	6	20	10	6	10	7	8	3	10	4	4	4	2
Selenopemphix quanta	0	4	0	2	2	2	3	1	3	2	1	2	0
Spiniferites elongatus	4	6	6	3	2	8	7	5	4	7	10	6	2
Spiniferites ramosus	0	6	2	5	2	3	1	2	4	2	1	2	3
Spiniferites mirabilis-hyperacanthus	0	0	0	0	0	0	0	0	1	0	0	0	0
Spiniferites spp.	1	2	0	0	0	0	3	0	4	2	2	1	0
Ataxiodinium choane	1	0	0	0	0	0	0	0	0	0	0	0	0
c.f Alexandrium tamarense type Kyste	0	0	0	0	0	0	0	0	0	0	0	0	0
Total	300	302	306	300	321	305	273	298	273	293	360	321	270

Tableau B.2.
Dénombrement des grains de pollen et des spores dans la carotte COR0503-CL05-37PC

	Profondeur (cm)	30	32	34	36	38	40	42	44	46	48	50	52	54	56
Pollen	*Abies*	6	9	3	6	6	12	9	1	8	5	5	0	4	8
	Picea	225	247	220	300	300	405	188	160	176	163	184	161	193	260
	Pinus	153	161	86	166	167	255	107	62	98	114	79	112	67	75
	Tsuga	10	10	1	1	0	8	1	0	0	1	2	1	2	2
	Acer	8	0	0	0	0	0	1	0	0	0	2	0	2	7
	Quercus	15	5	0	9	8	4	3	0	0	1	2	2	1	0
	Betula	32	28	34	26	25	37	20	8	6	6	9	5	15	6
	Alnus spp.	2	0	0	3	0	4	0	0	2	0	2	0	0	2
	Alnus type *crispa*	5	0	6	1	0	4	1	3	1	1	1	0	1	1
	Salix	7	4	4	9	2	7	0	2	3	0	0	0	1	0
	Type *Ambrosia*	6	7	3	4	2	2	2	0	1	0	0	0	3	1
	Artemisa	0	0	0	2	0	2	0	0	0	0	0	0	0	0
	Type *Rumex*	0	0	0	0	0	0	0	0	0	0	0	0	0	0
	Indéterminés	2	6	12	6	4	17	3	3	4	2	11	2	4	0
Spores	*Lycppodium annotium*	7	9	3	2	0	5	0	0	1	2	2	0	1	1
	Lycppodium clavatum	2	9	8	10	8	3	3	0	1	1	5	0	2	0
	Lycppodium lucidulum	0	0	0	0	0	0	0	0	0	0	1	0	1	1
	Spore monolète	14	10	12	15	2	14	11	3	6	2	1	9	5	3
	Spore trilète	23	16	13	21	6	10	4	1	1	1	0	2	5	5
	Sphagnum	11	4	13	8	18	10	11	3	5	3	3	3	7	5
	Selaginella	0	0	0	0	0	0	0	0	0	0	0	1	0	0
	Total	528	525	418	589	548	799	364	246	313	302	309	298	314	377

Tableau B.2. (Suite)
Dénombrement des grains de pollen et des spores dans la carotte COR0503-CL05-37PC

	Profondeur (cm)	58	60	62	64	66	68	70	72	74	76	78	80	82	84
Pollen	*Abies*	8	11	6	2	10	10	3	2	4	5	4	3	1	0
	Picea	150	155	164	156	169	151	180	182	171	190	192	184	177	185
	Pinus	20	66	68	80	91	94	76	84	81	114	86	97	122	94
	Tsuga	0	4	1	3	0	1	0	1	1	1	3	1	0	0
	Acer	0	11	5	2	0	1	0	1	2	3	3	6	1	1
	Quercus	0	2	5	0	0	0	5	1	5	3	0	0	1	1
	Betula	8	40	35	32	20	24	21	13	15	18	46	25	20	28
	Alnus spp.	2	0	1	0	0	0	0	6	0	2	0	0	2	2
	Alnus type *crispa*	0	1	1	2	2	4	2	0	2	1	0	1	2	0
	Salix	0	0	1	0	0	0	0	0	0	2	3	2	0	0
	Type *Ambrosia*	3	10	8	5	3	3	0	6	3	2	0	2	1	1
	Artemisa	0	0	3	1	0	0	0	0	5	1	0	0	1	1
	Type *Rumex*	0	0	0	0	0	0	0	0	0	0	0	0	0	0
	Indéterminés	2	5	2	3	12	5	2	4	8	3	4	12	10	0
Spores	*Lycppodium annotium*	0	0	2	0	0	0	0	0	0	0	1	0	0	0
	Lycppodium clavatum	1	4	4	1	8	0	6	4	3	4	4	3	7	2
	Lycppodium lucidulum	2	1	3	2	0	0	0	2	0	0	1	1	2	1
	Spore monolète	1	4	4	2	4	0	2	5	3	3	3	2	0	2
	Spore trilète	1	1	2	1	0	0	0	0	0	0	1	3	0	0
	Sphagnum	6	4	6	10	5	10	5	6	6	6	10	3	14	12
	Selaginella	0	0	0	0	0	0	2	0	2	0	0	0	0	0
	Total	204	319	321	302	324	303	304	317	311	358	361	345	361	330

Tableau B.2. (suite)
Dénombrement des grains de pollen et des spores dans la carotte COR0503-CL05-37PC

	Profondeur (cm)	86	88	90	92	94	96	98	100	104	108	112	116	120	124
Pollen	*Abies*	1	0	0	0	0	0	0	0	0	1	1	0	0	0
	Picea	203	179	195	174	171	165	189	181	151	188	176	186	165	200
	Pinus	106	96	117	121	105	116	87	101	101	96	114	108	112	103
	Tsuga	1	0	3	0	3	1	2	0	0	1	0	1	0	0
	Acer	3	2	3	1	3	5	6	5	2	0	0	1	0	3
	Quercus	2	2	0	2	0	3	1	3	3	0	2	2	1	0
	Betula	17	15	21	19	11	11	32	14	36	21	15	14	11	14
	Alnus spp.	2	3	1	1	1	1	1	0	1	2	0	2	1	0
	Alnus type *crispa*	3	6	3	0	1	4	1	2	6	1	2	0	0	0
	Salix	1	2	3	0	0	0	2	2	0	0	0	0	0	1
	Type *Ambrosia*	0	3	4	0	0	1	3	2	10	6	3	2	1	0
	Artemisa	1	0	0	0	0	0	0	0	0	0	2	0	0	0
	Type *Rumex*	0	0	0	0	0	0	4	0	1	3	0	0	0	0
	Indéterminés	5	12	5	9	10	20	32	34	33	26	31	36	33	24
Spores	*Lycppodium annotium*	0	0	0	0	0	0	0	0	0	0	0	0	0	0
	Lycppodium clavatum	8	3	4	3	6	2	4	1	1	6	1	1	0	0
	Lycppodium lucidulum	2	1	0	1	0	0	2	1	1	0	3	2	0	0
	Spore monolète	2	2	4	1	3	1	5	1	0	3	0	0	2	1
	Spore trilète	0	0	0	0	0	0	0	0	0	0	0	0	0	0
	Sphagnum	6	7	11	20	19	10	6	10	34	3	11	16	4	8
	Selaginella	0	0	0	0	0	0	0	0	0	0	0	0	0	0
	Total	363	333	374	352	333	340	377	357	380	357	361	371	330	354

Tableau B.2. (suite)
Dénombrement des grains de pollen et des spores dans la carotte COR0503-CL05-37PC

	Profondeur (cm)	128	132	136	140	144	148	152	156	160	164	168	172	176
Pollen	*Abies*	0	0	0	0	0	1	0	0	0	0	0	0	0
	Picea	148	203	192	179	172	276	203	207	166	178	166	176	220
	Pinus	124	84	105	160	102	114	56	74	100	95	97	90	116
	Tsuga	0	0	0	0	0	0	0	0	1	0	0	0	0
	Acer	0	2	0	1	1	5	0	6	2	0	0	0	0
	Quercus	0	0	0	0	0	0	0	0	0	0	1	4	1
	Betula	22	20	21	21	16	26	21	15	22	21	20	28	22
	Alnus spp.	0	0	0	2	0	0	0	1	1	0	0	0	0
	Alnus type *crispa*	0	0	1	4	3	3	0	2	0	0	0	0	0
	Salix	1	0	1	1	0	1	2	3	0	0	0	0	0
	Ambrosia	2	0	0	5	0	4	4	1	0	3	0	0	0
	Artemisa	0	0	0	0	0	0	0	1	0	0	0	0	0
	Type *Rumex*	0	0	0	0	0	0	0	0	0	0	0	0	0
	Indéterminés	31	11	4	2	3	14	21	4	12	16	10	12	14
Spores	*Lycppodium annotium*	0	1	1	0	0	2	0	1	6	3	1	1	0
	Lycppodium clavatum	1	6	5	4	5	3	2	2	0	0	1	2	1
	Lycppodium lucidulum	0	0	0	3	4	0	0	0	1	0	0	0	0
	Spore monolète	1	0	0	0	2	1	0	1	2	0	1	1	0
	Spore trilète	0	0	0	0	0	0	0	0	0	0	0	0	0
	Sphagnum	13	13	11	11	3	13	1	3	10	8	4	5	9
	Selaginella	0	0	0	0	0	0	0	0	0	0	0	0	0
	Total	343	340	341	393	311	463	310	321	323	324	301	319	383

Tableau B.3.
Dénombrement des palynomorphes remaniés et des réseaux organiques dans la carotte COR0503-CL05-37PC

Profondeur (cm)	30	32	34	36	38	40	42	44	46	48	50	52	54	56
Halodinium	30	30	15	21	21	42	44	29	33	18	17	12	9	26
Pédiastrum	0	0	0	0	0	6	0	0	0	0	0	0	0	3
Réseaux organiques	122	89	63	104	99	92	76	32	84	51	40	43	42	51

Profondeur (cm)	58	60	62	64	66	68	70	72	74	76	78	80	82	84
Halodinium	16	17	13	13	18	11	8	21	14	11	22	21	20	23
Pédiastrum	1	0	0	0	0	0	0	0	0	0	0	0	0	0
Réseaux organiques	64	61	50	54	64	62	40	52	72	62	67	91	74	63

Profondeur (cm)	86	88	90	92	94	96	98	100	104	108	112	116	120	124
Halodinium	25	20	30	31	34	22	11	17	8	15	10	17	9	24
Pédiastrum	0	0	0	0	0	0	0	0	0	0	0	0	0	0
Réseaux organiques	95	74	78	73	90	72	88	97	58	106	101	104	112	107

Profondeur (cm)	128	132	136	140	144	148	152	156	160	164	168	172	176
Halodinium	11	2	2	2	4	7	4	5	10	5	4	2	4
Pédiastrum	0	0	0	0	0	0	0	0	0	0	0	0	0
Réseaux organiques	94	66	101	91	92	99	61	51	56	42	42	40	43

Tableau B.4.
Dénombrement des foraminifères benthiques dans la carotte COR0503-CL05-37PC

Profondeur (cm)	30	32	34	36	38	40	42	44	46	48	50	52	54	56
Bolivina inflata	0	0	0	0	0	1	0	0	0	0	0	0	1	0
Brizalina subaenariensis	1	1	0	1	1	1	1	0	2	0	0	1	1	2
Bucella frigida	0	2	1	3	7	5	0	1	3	2	6	0	1	4
Bulimina exilis	2	8	10	14	22	25	11	16	21	14	16	31	20	30
Bulimina marginata	10	14	9	14	16	21	12	23	21	9	12	10	14	13
Cassidulina reniforme	0	0	0	0	0	1	1	0	0	0	0	0	0	0
Cibicides lobatulus	0	0	0	0	0	0	0	0	0	0	0	0	0	1
Cibicides pseudoungerianus	0	0	0	0	0	0	0	0	0	0	0	0	0	0
Dentalina sp.	0	0	0	0	0	0	0	0	0	0	0	0	0	1
Elphidium excavatum	4	3	3	6	4	7	3	5	1	5	4	7	5	4
Fissurina sp.	0	0	0	1	1	0	0	0	0	0	0	0	0	0
Glandulina laevigata	0	0	1	0	0	0	1	2	0	0	2	2	0	2
Globobullimina auriculata	0	6	3	5	7	4	1	5	3	2	1	4	0	2
Islandiella norcrossi	0	0	0	0	0	1	0	0	0	0	0	0	0	0
Lagena sp.	1	0	3	4	3	3	0	2	3	1	3	2	2	4
Lenticulina sp.	0	1	0	0	0	1	1	1	0	0	0	0	0	0
Nanionellina labradorica	3	9	1	9	8	5	7	12	6	5	13	19	9	11
Nonionellina turgida	0	0	0	1	0	1	0	0	1	0	0	0	0	0
Oolina hexagona	0	1	0	0	0	0	0	0	0	0	0	0	0	0
Oridorsalis umbonatus	0	0	0	1	0	2	0	0	0	0	0	0	1	1
Quinqueloculina seminulum	0	0	0	0	0	0	0	0	0	0	0	0	2	0
Indéterminés	0	0	0	0	0	0	0	0	0	0	0	0	0	0
Total	21	45	31	59	69	78	38	67	61	38	57	76	56	75

Tableau B.4. (suite)
Dénombrement des foraminifères benthiques dans la carotte COR0503-CL05-37PC

Profondeur (cm)	58	60	62	64	66	68	70	72	74	76	78	80	82	84
Bolivina inflata	0	1	0	0	0	0	0	1	0	0	0	0	0	0
Brizalina subaenariensis	0	1	1	1	3	0	2	6	3	1	0	0	1	2
Bucella frigida	8	2	5	1	0	3	0	6	9	1	0	1	1	0
Bulimina exilis	22	29	22	35	22	24	9	30	72	8	16	9	5	14
Bulimina marginata	30	12	12	19	19	15	3	41	75	11	12	18	14	25
Cassidulina reniforme	2	0	0	2	1	0	0	0	0	0	0	0	0	0
Cibicides lobatulus	0	0	1	0	0	0	0	0	1	0	0	0	0	0
Cibicides pseudoungerianus	0	0	0	0	0	0	0	0	0	0	0	0	0	0
Dentalina sp.	1	1	0	0	0	1	0	0	0	0	3	0	0	1
Elphidium excavatum	8	11	11	5	7	4	5	16	26	10	0	8	4	5
Fissurina sp.	0	0	0	0	0	0	0	0	0	0	0	0	0	0
Glandulina laevigata	1	1	1	1	1	2	0	3	0	0	1	1	0	0
Globobullimina auriculata	3	3	2	7	6	9	0	11	12	1	4	7	2	2
Islandiella norcrossi	0	0	1	1	0	0	0	2	2	0	0	1	0	0
Lagena sp.	2	6	1	3	1	1	0	1	4	2	0	2	2	2
Lenticulina sp.	1	0	0	0	0	0	0	1	0	0	0	1	0	0
Nanionellina labradorica	14	8	3	4	3	7	0	4	14	2	3	5	2	2
Nanionellina turgida	1	1	1	0	0	0	0	0	0	0	0	0	0	0
Oolina hexagona	0	0	0	0	1	0	0	0	0	0	0	0	0	0
Oridorsalis umbonatus	2	0	0	0	1	0	0	0	0	0	0	0	0	0
Quinquoloculina seminulum	0	0	0	0	0	0	0	0	0	0	0	0	0	0
Indéterminés	1	1	0	0	0	0	0	0	0	0	0	0	0	0
Total	96	77	61	79	65	66	19	122	218	36	39	53	31	53

Tableau B.4. (suite)
Dénombrement des foraminifères benthiques dans la carotte COR0503-CL05-37PC

Profondeur (cm)	86	88	90	92	94	96	98	100	104	108	112	116	120	124
Bolivina inflata	0	0	0	0	0	0	0	0	0	0	0	0	0	0
Brizalina subaenariensis	2	1	0	0	0	0	0	0	0	0	0	0	0	0
Bucella frigida	0	0	0	0	0	1	0	0	0	0	0	0	0	0
Bulimina exilis	10	10	8	3	10	21	15	16	11	4	0	11	11	7
Bulimina marginata	26	25	10	3	18	24	22	12	24	0	2	4	8	1
Cassidulina reniforme	0	0	0	0	0	0	0	1	0	0	0	0	1	0
Cibicides lobatulus	0	0	0	0	0	0	0	0	0	1	0	0	0	0
Cibicides pseudoungerianus	0	0	0	0	0	0	0	0	0	0	0	0	0	0
Dentalina sp.	0	0	0	0	0	0	0	0	0	0	0	0	0	1
Elphidium excavatum	3	3	0	0	1	5	12	4	16	5	0	4	8	7
Fissurina sp.	0	0	0	0	0	0	0	0	0	0	0	0	0	0
Glandulina laevigata	1	0	0	0	0	1	0	0	0	0	0	0	0	0
Globobullimina auriculata	2	1	0	0	1	3	10	1	4	1	0	0	0	0
Islandiella norcrossi	1	1	0	0	3	10	4	4	14	0	0	0	0	0
Lagena sp.	3	0	0	0	3	2	2	3	1	1	0	0	0	2
Lenticulina sp.	0	0	0	0	0	0	0	0	0	0	0	0	0	0
Nanionellina labradorica	4	6	4	1	11	15	25	7	36	7	1	6	3	0
Nonionellina turgida	0	0	0	0	0	0	0	0	0	0	0	0	0	0
Oolina hexagona	0	0	1	0	0	0	0	0	0	0	0	0	0	0
Oridorsalis umbonatus	0	0	0	0	0	0	0	1	0	0	0	0	0	0
Quinquoloculina seminulum	0	0	0	0	0	0	0	0	0	0	0	0	0	0
Indéterminés	0	0	0	0	0	0	0	0	0	0	0	0	0	0
Total	52	47	23	7	47	82	90	49	106	19	3	25	31	18

Tableau B.4. (suite)
Dénombrement des foraminifères benthiques dans la carotte COR0503-CL05-37PC

Profondeur (cm)	128	132	136	140	144	148	152	156	160	164	168	172	176
Bolivina inflata	0	0	0	0	0	1	0	0	0	0	0	0	0
Brizalina subaenariensis	0	1	0	0	0	1	1	1	1	0	0	0	0
Bucella frigida	0	0	0	0	0	0	0	0	0	0	0	0	0
Bulimina exilis	9	25	11	23	23	18	27	22	29	0	27	34	18
Bulimina marginata	3	12	6	21	12	5	15	29	10	5	7	13	10
Cassidulina reniforme	0	0	0	0	0	0	0	0	0	0	0	0	0
Cibicides lobatulus	0	0	0	0	0	1	0	0	1	1	0	0	0
Cibicides pseudoungerianus	2	2	0	0	0	0	1	0	0	0	0	0	0
Dentalina sp.	0	0	0	0	0	0	1	0	0	1	0	0	0
Elphidium excavatum	3	9	0	8	2	7	6	2	2	0	1	3	1
Fissurina sp.	0	0	0	0	0	0	0	0	0	0	0	0	0
Glandulina laevigata	0	2	1	0	0	1	1	0	1	1	0	2	0
Globobullimina auriculata	0	0	0	0	1	0	0	0	0	0	0	0	0
Islandiella norcrossi	0	0	0	0	1	1	0	0	0	0	0	0	0
Lagena sp.	0	4	0	0	0	0	0	2	0	1	1	3	0
Lenticulina sp.	0	0	0	0	0	0	1	0	0	1	0	0	0
Nanionellina labradorica	1	0	1	1	4	2	3	2	1	1	0	1	0
Nonionellina turgida	0	0	0	0	0	0	0	0	0	0	0	0	0
Oolina hexagona	1	1	0	0	0	0	0	0	0	0	0	0	0
Oridorsalis umbonatus	2	2	0	0	0	0	0	1	0	0	0	0	0
Quinquoloculina seminulum	0	0	0	0	0	0	1	0	0	1	1	1	0
Indéterminés	0	0	0	0	0	0	0	0	0	0	0	0	0
Total	21	58	19	53	43	37	57	59	45	12	37	57	29

Tableau B.5.
Concentrations des palynomorphes dans la carotte COR0503-CL05-37PC

Profondeur (cm)	30	32	34	36	38	40	42	44	46	48	50	52	54	56
Dinokystes (nb /cm^3)	5742	6757	5511	6799	6559	6992	6039	12712	4268	5047	6848	5874	9063	6788
Pollen (nb /cm^3)	8753	11220	6756	12079	11237	21154	19155	10094	16105	18149	15769	14814	23673	21700
Spores (nb /cm^3)	1059	1129	897	1269	743	1174	1658	296	754	557	637	785	1697	899
Réseaux organiques (nb /cm^3)	2267	2005	1153	2357	2164	2137	1765	1351	1363	998	1018	918	1369	1316
Halodinium (nb /cm^3)	557	676	275	476	459	976	1022	1225	536	352	433	256	293	671
Pédiastrum (nb /cm^3)	0	0	0	0	0	139	0	0	0	0	0	0	0	77
Foraminifères benthiques calcaires (nb /cm^3)	2	3	3	4	5	5	3	4	4	3	5	5	4	5

Profondeur (cm)	58	60	62	64	66	68	70	72	74	76	78	80	82	84
Dinokystes (nb /cm^3)	8321	6707	7038	7110	6863	7852	7610	4985	7582	9699	6719	6927	9353	7556
Pollen (nb /cm^3)	10247	11808	6969	18016	15630	27922	14133	10559	14152	20035	16248	20977	22432	18176
Spores (nb /cm^3)	584	542	488	1008	866	953	734	598	667	755	953	756	1526	987
Réseaux organiques (nb /cm^3)	1775	1359	1161	1247	1459	1623	1011	861	1784	1873	1407	2001	2292	1551
Halodinium (nb /cm^3)	444	379	302	300	410	288	202	348	347	332	462	462	619	566
Pédiastrum (nb /cm^3)	28	0	0	0	0	0	0	0	0	0	0	0	0	0
Foraminifères benthiques calcaires (nb /cm^3)	6	5	4	5	4	5	4	8	15	3	3	5	2	4

Tableau B.5. (suite)
Concentrations des palynomorphes dans la carotte COR0503-CL05-37PC

Profondeur (cm)	86	88	90	92	94	96	98	100	104	108	112	116	120	124
Dinokystes (nb /cm^3)	9232	14676	11260	8383	9695	15065	8568	7556	15692	12416	9657	9409	9218	11707
Pollen (nb /cm^3)	26713	33980	35659	20255	17712	39204	20906	18264	20621	53426	24263	42201	31689	30529
Spores (nb /cm^3)	1394	1380	1909	1549	1626	1559	987	690	2158	1858	1052	2278	587	796
Réseaux organiques (nb /cm^3)	2847	3526	2870	1980	2909	3769	2497	2387	2994	4329	3077	3068	3278	3977
Halodinium (nb /cm^3)	749	953	1104	841	1099	1152	312	418	413	613	305	501	263	892
Pédiastrum (nb /cm^3)	0	0	0	0	0	0	0	0	0	0	0	0	0	0
Foraminifères benthiques calcaires (nb /cm^3)	3	3	2	1	3	5	6	4	7	2	1	2	2	1

Profondeur (cm)	128	132	136	140	144	148	152	156	160	164	168	172	176
Dinokystes (nb /cm^3)	14295	8376	10246	6559	11150	11336	8823	10255	7352	9810	9356	10558	10790
Pollen (nb /cm^3)	24878	16990	24084	19357	23486	30559	18111	18823	15065	19070	13325	12802	27506
Spores (nb /cm^3)	1138	1062	1264	929	1107	1308	177	420	942	670	317	372	737
Réseaux organiques (nb /cm^3)	4479	1831	3382	1989	3196	3679	1971	1755	1508	1406	1092	1316	1718
Halodinium (nb /cm^3)	524	55	67	44	139	260	129	172	269	167	104	66	160
Pédiastrum (nb /cm^3)	0	0	0	0	0	0	0	0	0	0	0	0	0
Foraminifères benthiques Calcaires (nb /cm^3)	1	4	1	4	3	3	6	4	3	1	3	4	3

ANNEXE C

Planches photographiques des foraminifères benthiques calcaires dans la carotte COR0503-CL05-37PC prises par microscope électronique à balayage

Planches photographiques :

Planche 1

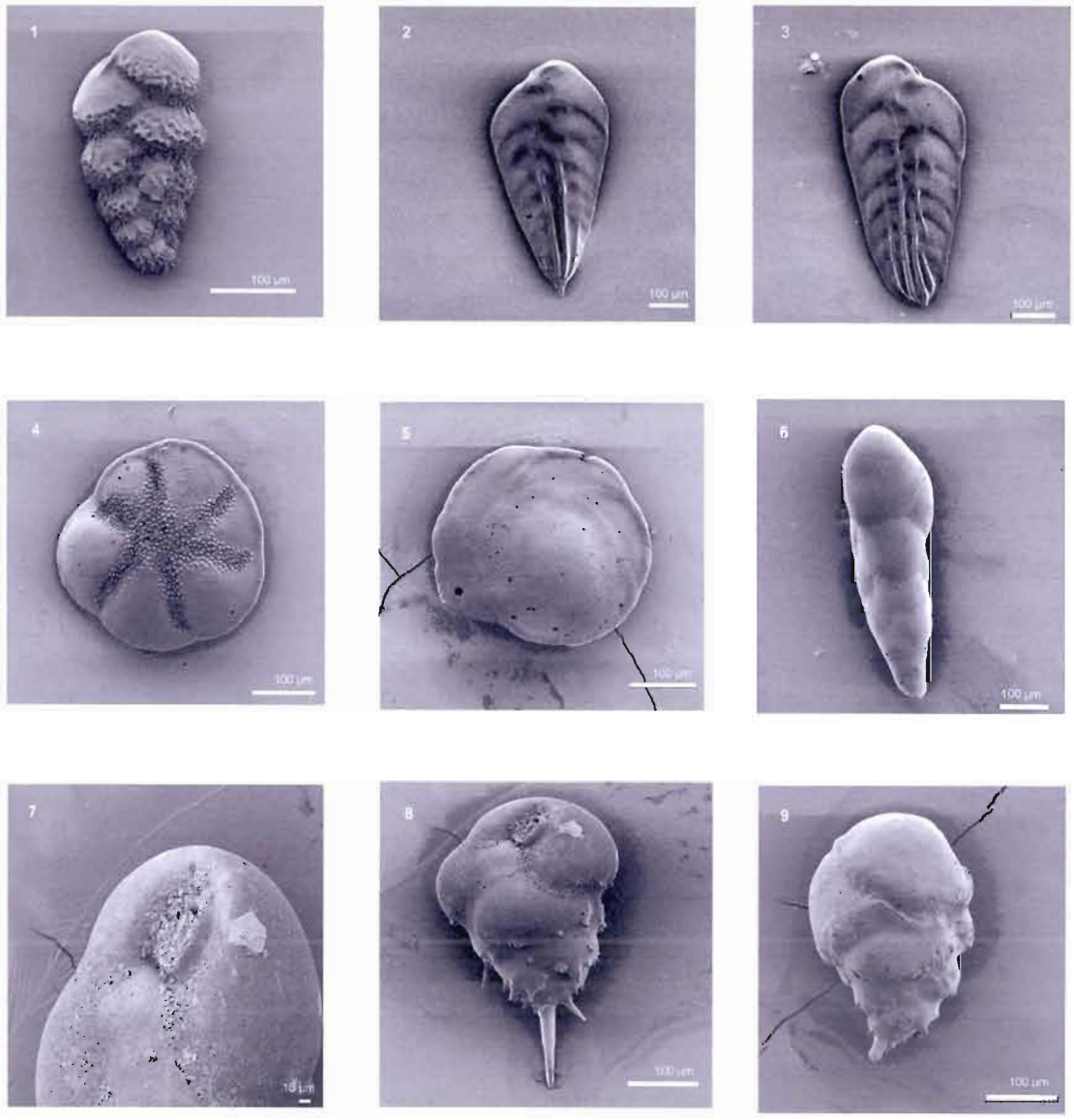

Planche 1 : Photographies au microscope électronique à balayage des foraminifères benthiques calcaires prélevés dans la carottes COR0503-CL05-37PC

Planche 2

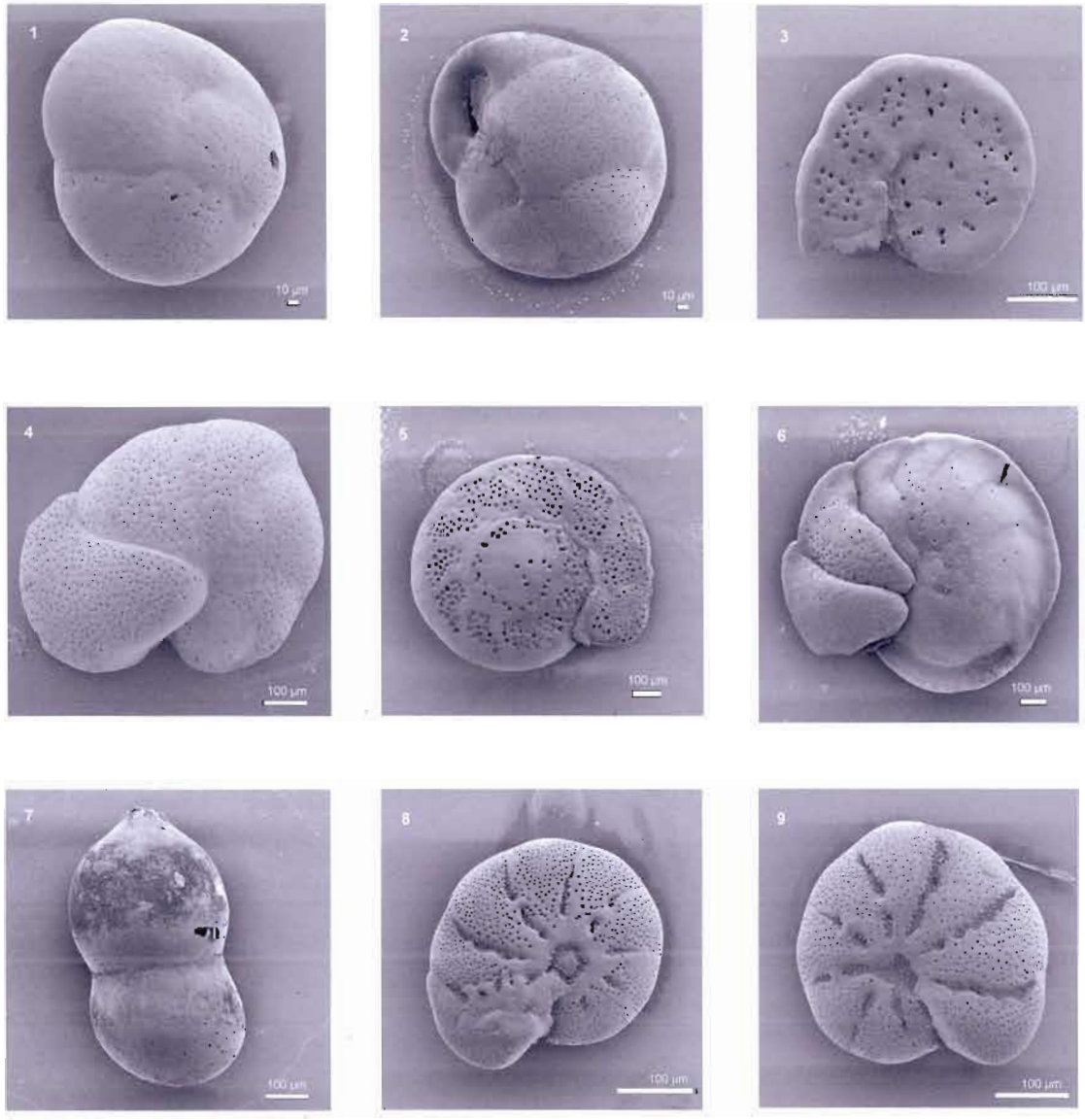

Planche 2: Photographies au microscope électronique à balayage des foraminifères benthiques calcaires prélevés dans la carottes COR0503-CL05-37PC

Planche 3

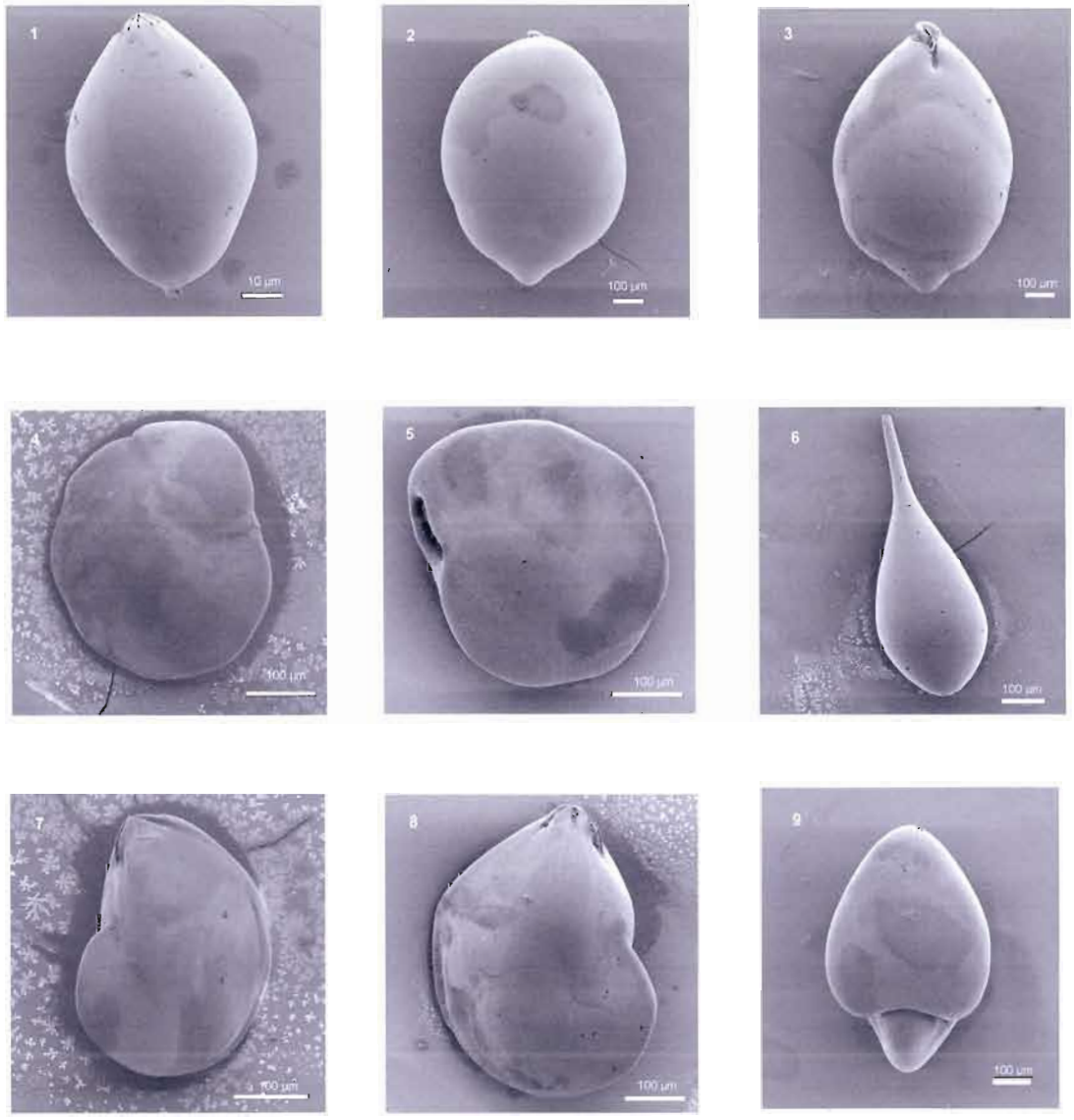

Planche 3: Photographies au microscope électronique à balayage des foraminifères benthiques calcaires prélevés dans la carottes COR0503-CL05-37PC

Planche 4

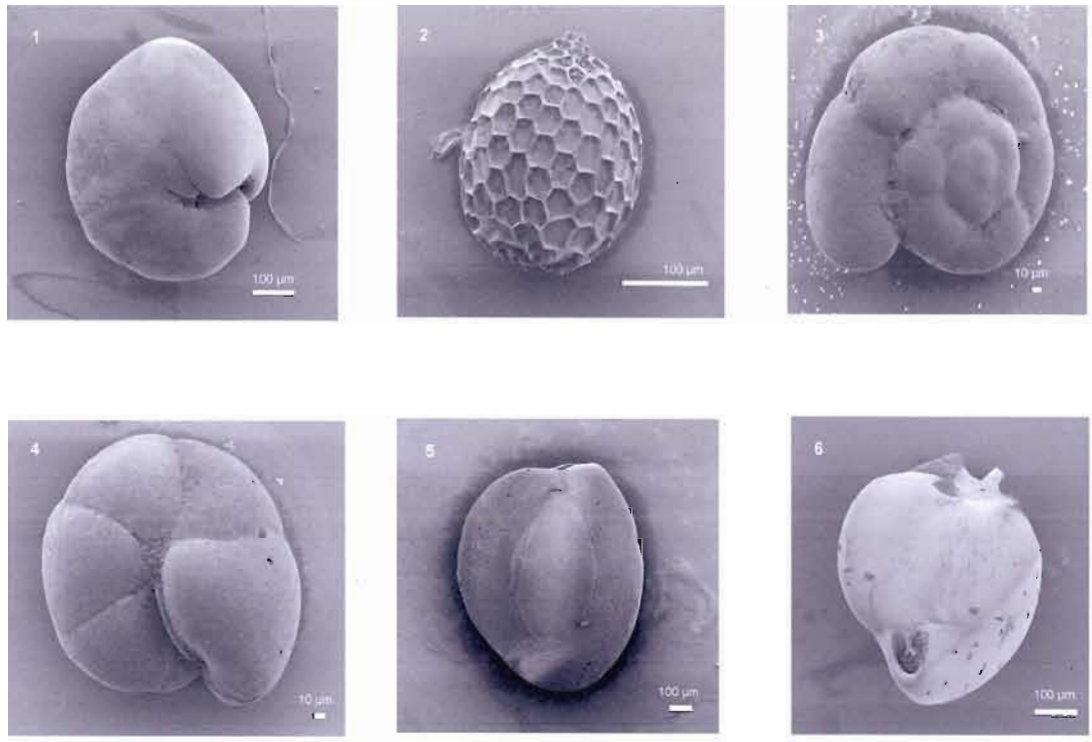

Planche 4: Photographies au microscope électronique à balayage des foraminifères benthiques calcaires prélevés dans la carottes COR0503-CL05-37PC

Légendes des planches

Planche 1:

* **Figure 1** *Bolivina inflata* (Heron-Allen and Earland, 1913)
* **Figures 2-3** *Brizalina subaenariensis* (Cushman, 1922)
  Fig. 2 vue dorsale
  Fig. 3 vue ventrale
* **Figures 4-5** *Buccella frigida* (Cushman, 1922)
  Fig. 4 vue dorsale
  Fig. 5 vue ventrale
* **Figure 6** *Bulimina exilis* (Whitelegge, 1907)
* **Figures 7-8-9** *Bulimina marginata* (d'Orbigny 1826)
  Fig. 7 vue aperturale
  Fig. 8 vue ventrale
  Fig. 9 vue dorsale

Planche 2 :

* **Figures 1-2** *Cassidulina reniforme* (Nørvang, 1945)
  Fig. 1 vue dorsale
  Fig. 2 vue ventrale
* **Figures 3-4** *Cibicides lobatulus* (Walker and Jacob 1798)
  Fig. 3 vue dorsale
  Fig. 4 vue ventrale
* **Figures 5-6** *Cibicides pseudoungerianus* (Cushman, 1922)
  Fig. 5 vue dorsale
  Fig. 6 vue ventrale
* **Figure** 7 *Dentalina* sp.
* **Figures 8-9** *Elphidium excavatum* (Terquem 1876)

Planche 3 :

* **Figure 1** *Glandulina laevigata* (d'Orbigny 1846)
* **Figures 2-3** *Globobulimina auriculata* (Bailey, 1851)
* **Figures 4-5** *Islandiella norcrossi* (Cushman, 1933)
  Fig. 4 vue dorsale
  Fig. 5 vue ventrale
* **Figure 6** *Lagena* sp.
* **Figures 7-8** *Lenticulina* sp.

* **Figure 9** *Nonionellina labradorica* (Dawson, 1860)

Planche 4 :

* **Figure 1** *Nonionellina labradorica* (Dawson, 1860)
* **Figure 2** *Oolina hexagona* (Williamson, 1848)
* **Figures 3-4** *Oridorsalis umbonatus* (Reuss, 1851)
  Fig. 3 vue dorsale
  Fig. 4 vue ventrale
* **Figures 5-6** *Quinqueloculina seminulum* (Linné, 1758)
  Fig. 5 vue générale
  Fig. 6 vue apicale